Chapter 6

Changes of Permanent Lake Surfaces, and Their Consequences for Dust Aerosols and Air Quality: The Hamoun Lakes of the Sistan Area, Iran

Alireza Rashki, Dimitris Kaskaoutis, C.J.deW. Rautenbach and Patrick Eriksson

Additional information is available at the end of the chapter

http://dx.doi.org/10.5772/48776

1. Introduction

Changes in the frequency and extent of natural inundation occurring on large permanent and ephemeral lake systems may lead to significant fluctuations in regional dust loading on both a seasonal and an inter-annual basis [1]. As surface water diversion increases, arid-land surfaces that were previously wet or stabilized by vegetation are increasingly susceptible to deflation by wind, resulting in desertification and increase in dust outbreaks [2-4]. Desiccation of lake beds, whether due to drought or to water diversion schemes, as in the Aral Sea in Turkmenistan [5,6], Owens lake in California [7,8], lake Eyre in Australia, Hamoun lakes in Iran [9-12], can lead to increased dust storm activity. Thus, some dust may be derived from dried lake beds and can be highly saline, while the finest aerosols can be injurious to health. Anthropogenic sources were previously considered as important dust contributors [13], but more recent estimates of only 5-7% of total mineral dust from such sources gives major importance to natural sources [14]. Each year, several billion tons of soil-dust are entrained into the atmosphere playing a vital role in solar irradiance attenuation, and affects marine environments, atmospheric dynamics and weather [15-20].

Atmospheric aerosols affect the global climatic system in many ways, i.e. by attenuating the solar radiation reaching the ground, modifying the solar spectrum, re-distributing the earth-atmosphere energy budget and influencing cloud microphysics and the hydrological cycle. Mineral dust plays an important role in the optical, physical and chemical processes in the atmosphere, while dust deposition adds exogenous mineral and organic material to terrestrial surfaces, having a significant impact on the Earth's ecosystems and biogeochemical cycles. The impact of dust aerosols in the Earth's system depends mainly on particle characteristics such as size, shape and mineralogy [21], which are initially determined by the terrestrial sources from which the soil sediments are entrained and from

their chemical composition [22]. Size distribution is a key parameter to characterize the aerosol chemical, physical, optical properties and their effects on health. The lower and upper size limits of dust aerosols are from a few nanometers to ~100μm and aerosol properties change substantially over this size range. Several studies demonstrated that airborne Particulate Matter (PM) has an impact on climate [23], biogeochemical cycling in ecosystems [24], visibility [25] and human health [26-28]. Over recent years in the public health domain the PM concentration has become a topic of considerable importance, since epidemiological studies have shown that exposure to particulates with aerodynamic diameters of < 10 μm (PM_{10}) and especially < 2.5 μm ($PM_{2.5}$) induces an increase of lung cancer, morbidity and cardiopulmonary mortality [e.g. 29-35]. Thus air pollution appears to have an adverse effect on respiratory and cardiovascular systems [36], which might result in an acute reduction of lung function, aggravation of asthma, increased risk of pneumonia in the elderly, low birth weight and high death rates in newborns [37].

Some dust contaminants (soluble and chelatable metallic salts, pesticides, etc) affect human health when they are transported over densely populated areas [38], retained in residences and other occupied structures [39], and they also impact the nutrient loading of waters flowing from adjacent watersheds [40] and terminal bodies of water by direct and indirect deposition [41-42]. PM is a complex mixture of substances suspended in to the atmosphere in solid or liquid state with different properties (e.g. variable size distribution or chemical composition amongst others) and origins (anthropogenic and natural). Owing to this mixture of substances, the chemical composition of PM may vary widely as a function of emission sources and the subsequent chemical reactions which take place in the atmosphere [43-45].The chemical mass balance is the most commonly used method for assessing PM source contributions [46], while statistical methods, such as factor analysis and multi-linear regression [47], have also produced interesting results regarding dust source identification. Elemental and mineralogical analyses have also been used to identify the source regions of dust deposited in Arctic ice caps [48] and on other depositional surfaces [49, 42].

One spectacular example of such dust effects is the Hamoun (dry) lakes in the eastern part of Iran that has attracted scientific interest during recent years, since it constitutes a major dust source region in southwest Asia, often producing intense dust storms that cover the Sistan region in eastern of Iran and the southwest of Afghanistan and Pakistan and influencing the air quality, human health and ecosystems as well as aerosol loading and climate from local to regional scales [50-52, 12]. Particles from the Hamoun dust storms might also cover farm and grasslands to result in damage to crops and fill the rivers and water channels with aeolian material. Over recent years, tens of thousands of people have suffered from respiratory diseases and asthma during months of devastating dust storms in the Sistan basin, especially in the cities of Zabol and Zahak and the surrounding villages [53]. According to the Asthma Mortality Map of Iran, the rate of asthma in Sistan is, in general, higher than in other regions [54].

The aim of this Chapter is to: (1) assess the seasonal and annual variability of dust storms that originate from the Hamoun Basin, (2) identify the amount of dust loading from the dry lakes, (3) assess the contribution of the lake beds to regional dust emissions for specific locations, (4) assess the dust chemical and mineralogical composition to provide useful

information regarding the status of dust storms and also human health and, (5) assess dust concentrations and air quality of the regions affected by the dust storms.

2. Sistan region

The Sistan basin (Helmand basin) lies between the Hindu Kush Mountains in Afghanistan and the mountain ranges flanking the eastern border of Iran and is the depository that receives the discharge of the Helmand (Hirmand) river in the lower Sistan Basin (Fig. 1). It is a large and remote desert basin, extremely arid and known for its windstorms, extreme floods and droughts. The closed basin receives the waters of the Helmand river, the only major perennial river in western Asia between the Tigris-Euphrates and Indus rivers [9]. The Helmand and its tributary streams drain the southern Hindu Kush Mountains of Afghanistan and flow into an otherwise waterless basin of gravel plains and sandy tracts before terminating in Sistan (also Seistan, British spelling), a depression containing the large inland delta of the Helmand river and a series of shallow, semi-connected playas at the western edge of the basin (Fig. 1).

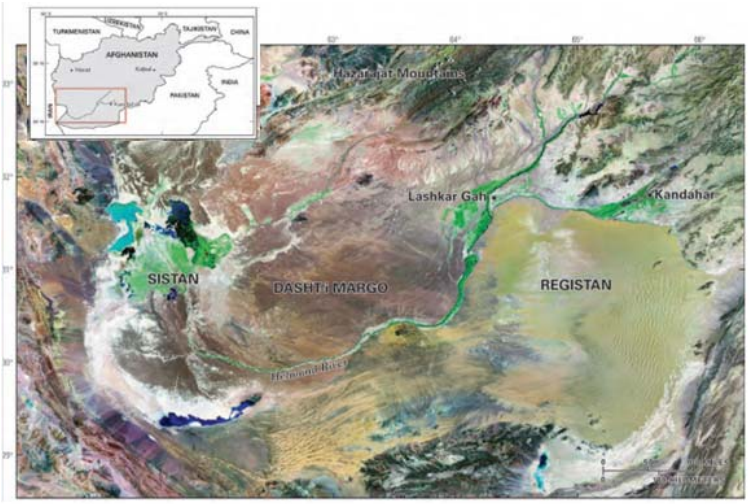

Figure 1. Landsat-5 image showing the lower Hirmand Basin and Sistan region. [9].

In 1949 the United States initiated a new program for the improvement of underdeveloped areas of the world. The damming of the Helmand river in southern Afghanistan became one of the showcase projects of U.S. foreign aid in the "Third World" after World War II. Dams were built on the Helmand river and its main tributary (Arghandab river) during the 1950s. The main project goals were to provide hydroelectric power and increase agricultural productivity through irrigation and land reclamation. The Arghandab dam, located northwest of the city of Kandahar, was completed in 1952 with a height of 145 feet (44.2 meters) and storage capacity of 388,000 acre-feet (478.6 million cubic meters). The larger Kajakai dam on the Helmand was completed a year later with a height of 300 feet (91.4 meters) and length of 919 feet (280 meters) and storage

capacity of 1,495,000 acre-feet (1,844 million cubic meters). About 300 miles (482.8 kilometers) of concrete-lined canals were built to distribute the reservoir waters [9]. The Hirmand river is the longest river in Afghanistan (ca. 1150 km; catchment > 160,000 km^2) and the main watershed for the Sistan basin, finally draining into the natural swamp of the Hamoun lakes complex [10].

Severe dust plumes usually extend from Sistan into southern Afghanistan and southwestern Pakistan obscuring the surface over much of the region (Fig 2). Severe droughts during the past decades, especially after 1999, have caused desiccation of the Hamoun lakes leaving a fine layer of sediment that is easily lifted by the wind [55], thus modifying the basin to one of the most active sources of dust in southwest Asia [56, 50, 57]. Therefore, the Hamoun dry-lake beds exhibit large similarities with the other two major dust source regions of the world that comprise of dried lakes and topographic lows, i.e. Bodele depression in Chad [3] and lake Eyre in Australia [4]. The strong winds blow fine sand off the exposed Hamoun lake beds and deposit it to form huge dunes that may cover a hundred or more villages along the former lakeshore. As a consequence, the wildlife around the lake has been negatively impacted and fisheries have been brought to a halt.

Fig. 2 (left panel) shows a severe dust storm over the Sistan region as observed from the Terra-MODIS satellite's true color image on 15 June 2004. The intense dust plumes form a giant U-shape extending from Sistan into southern Afghanistan and southwestern Pakistan that obscures the surface over much of the region. The pale color of the dust plume is consistent with that of dried wetland soils. The dust is blowing off the dry lake beds that become the Hamoun wetlands during wet years.

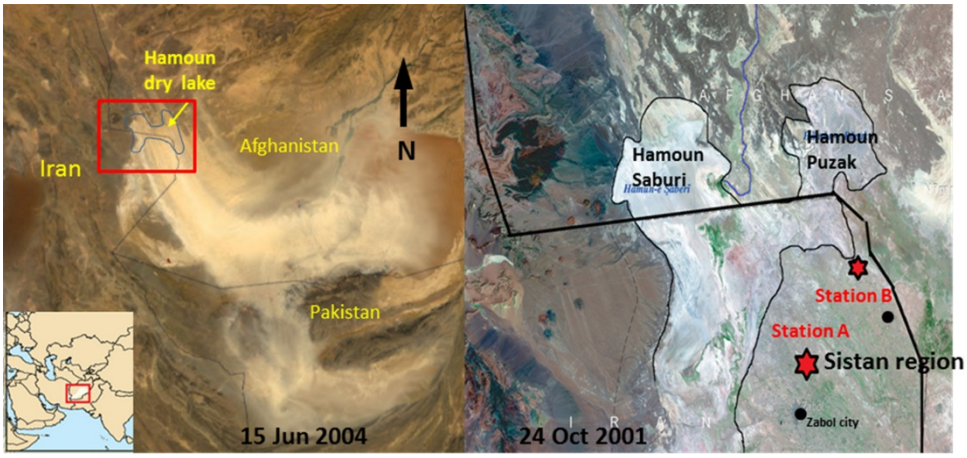

Figure 2. MODIS image of dust deflation over southern Afghanistan originating from the dry Hamoun lakes in Sistan on June 15, 2004.

3. Hamoun lakes

The Hamoun lakes are situated roughly at the termination of the Hirmand river's inland delta. The Hamoun lakes complex (Hamoun-e-Puzak, Hamoun-e-Sabori and Hamoun-e-Hirmand and Baringak) are located in the north of the Sistan region, which is also the largest fresh water ecosystem of the Iranian Plateau and one of the first wetlands in the Ramsar Convention [58]. Water in the Hamoun lakes is rarely more than 3 meters deep, while the size of the lakes varies both seasonally and from year to year. Maximum expansion takes place in late spring, following snowmelt and spring precipitation in the mountains. In years of exceptionally high runoff, the Hamoun lakes overflow their low divides and create one large lake that is approximately 160 kilometers long and 8–25 kilometers wide with nearly 4,500 square kilometres surface area. Overflow from this lake is carried southward into the normally dry Gaud-i Zirreh (Fig. 1), the lowest playa (463-meter altitude) in the Sistan depression. Furthermore, mountain runoff varies considerably from year to year; in fact, the Hamoun lakes have completely dried up at least three times in the 20th century [9]. The maximum extent of the Hamoun lakes following large floods is shown in Fig. 4, where a continuous large lake has been created covering an extended area of ~4,500 km^2 with a volume of 13000 million m^3 in Sistan and southwestern Afghanistan. This figure corresponds to spring of 1998 after snowmelt in the Afghanistan mountains that transferred large quantities of water into the Hamoun Basin. As a consequence, livelihoods in the Sistan region are strongly interlinked with and dependent on the wetland products and services, as well as on agricultural activities in the Sistan plain. Fishing and hunting represent an important source of income for many households and, therefore, the local and regional economy is strongly dependent on weather conditions, precipitation and land use – land cover changes. The political boundary between Iran and Afghanistan splits the Hamoun system, further complicating management possibilities in the area. Most (90%) of the watershed is located in Afghanistan and practically all of the wetlands' water sources originate there. The Iranian part is desert, and produces runoff only in rare cases of significant local rainfall [10].

In view of the Hirmand and the surrounding rivers that supply most of the sediments to the Hamoun lakes, a brief encapsulation of the relevant geology of the catchment area in Afghanistan is given. Afghanistan has a very complex geology, encompassing two major relatively young orogenies, Triassic and subsequent Himalayan, resulting in amalgamation of crustal blocks and formation of concomitant ophiolites and younger clastic and carbonate sedimentary rocks as well as basaltic lavas and, more recently, extensive alluvial and eolian detritus [59] . The Sistan region and Hamoun dry lake beds are mainly composed of Quaternary lacustrine silt and clay material as well as Holocene fluvial sand, silt and clay (Fig. 3). These materials have been carried to the basin by the rivers, while along their courses Neogene fluvial sand, eolian sand, silt and clay are the main constituents. Note also the difference in the soil-dust composition between two major desert areas, Registan and Dasht-i-Margo in Afghanistan. The former is composed of Neogene coarse gravels and the latter of Quaternary eolian sand. More details about the geology in the Sistan region can be found in [60].

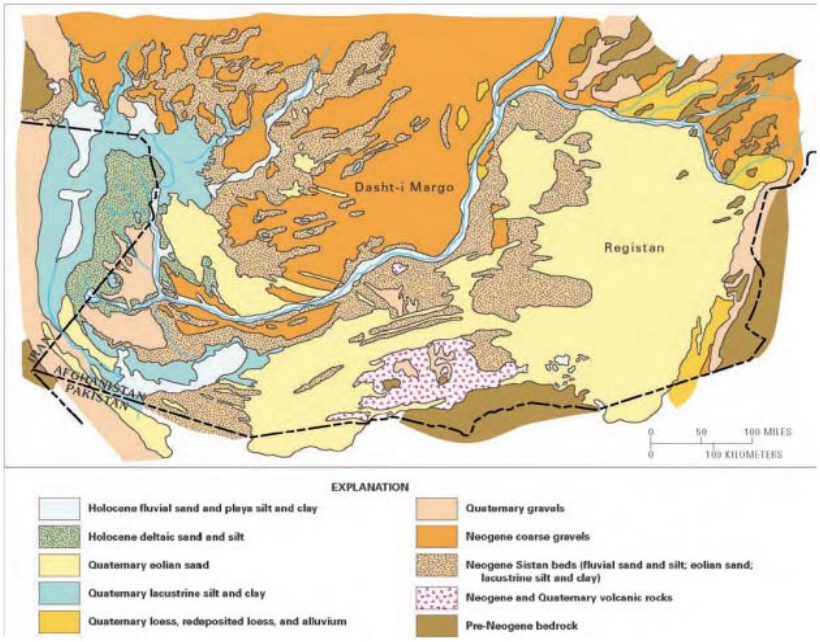

Figure 3. Geological map of the Sistan Basin and southern Afghanistan *[61-63].*

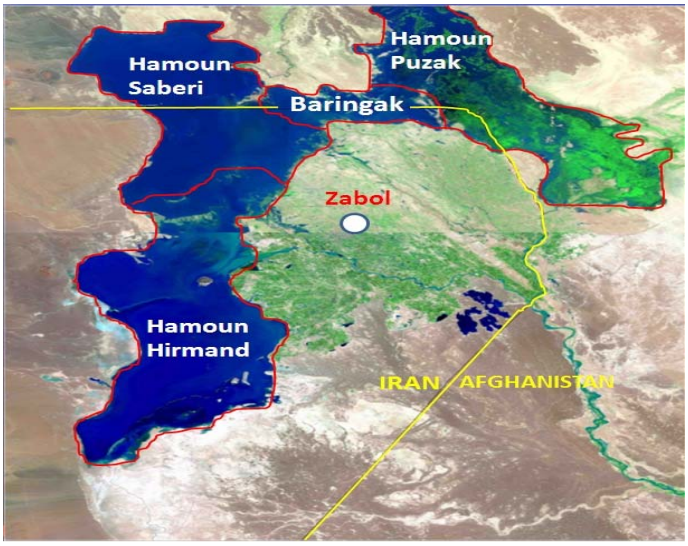

Figure 4. Position of the Hamoun Lakes in Iran and Afghanistan, showing a maximum inundation period.

4. Droughts in the Sistan

The Sistan Basin has recently experienced an unusually long 10-year drought starting in 2000 [10]. Combined with war and severe political disruption over the past 2 decades, the 10-year drought has created conditions of widespread famine that affected many people in eastern Iran and southwestern Afghanistan. A suggested, climatic forcing mechanism has been proposed for the recent drought by Barlow and others (2002). A prolonged ENSO (El Niño-Southern oscillation) cold phase (known as La Niña) from 1998 to 2001 and unusually warm ocean waters in the western Pacific appear to have contributed to the prolonged drought. The unusually warm waters (warm pool) resulted in positive precipitation anomalies in the Indian Ocean and negative anomalies over central Afghanistan [64], thus contributing to the drying of the Hamoun Basin. The contrast between a relatively wet year in 1976 and the nearly dry Hamoun lakes in 2001 is shown in Figs. 2 and 4. Millions of fish and untold numbers of wildlife and cattle died. Agricultural fields and approximately 100 villages were abandoned, and many succumbed to blowing sand and moving dunes [65].

Most of the Sistan population lives near the Hamoun lakes and is employed in agricultural, fishery, handicrafts and other jobs. To counter the effects of droughts, the Iranian government prepares facilities such as food and flour supplies, medicine and health services and employment in the region to prevent the forced emigration of people, but the continuous and extreme droughts have forced some people to leave the Sistan region. Long droughts at the end of the 1960s, middle of the 1980s, and from 1999 to 2010 affected the Sistan region significantly and resulted in desiccation of the Hamoun lakes, making the surrounding lands saline and disturbing their soil fertility, while some places became barren (see Fig. 5). The most important findings in Fig. 5 are: (1) in 1976, the Hamoun lakes were still thriving. Dense reed beds appear as dark green, while tamarisk thickets fringing the margins of the upper lakes show up as pink shades in the satellite images (Fig. 5). Bright green patches represent irrigated agricultural lands, mainly wheat and barley. The lakes flood to an average depth of half a meter, denoted by lighter shades of blue, while dark blue

Figure 5. Satellite (Landsat) images of the Hamoun Basin in spring of different years. Hamoun lakes are fed primarily by water catchments in neighbouring Afghanistan. In 1976, when rivers in Afghanistan were flowing regularly, the lake's water level was relatively high. Between 1999 and 2011, however, drought conditions caused frequent dryness of the Hamoun lakes that almost disappeared in 2001 after a 3-year intense drought period [65].

to black indicates deeper waters, which, however, do not exceed four meters. (2) By 2001, the Hamoun lakes had vanished since central and southwest Asia were hit by the largest persistent drought anywhere in the world. The only sign of water in this scorched landscape of extensive salt flats (white) is the Chah Nimeh reservoir in the southern part of Sistan (not shown on the satellite image), which is now only used for drinking water. Degraded reed stands in muddy soil are visible as dark green hues at the southern end of Hamoun-i Puzak. In 2003 the Hamoun Basin was covered with water again, but with significantly lower coverage than in the mid-1970s [65].

5. Data set and experimental methods

In order to address the scientific topics mentioned above multiple ground-based instrumentation and several sets of satellite images (mostly Landsat and MODIS) were used for illustration purposes and for detection of water level in Hamoun and for monitoring of land use – land cover changes, seasonality of dust storms and associated sediments, air quality perspectives, chemical and mineralogical composition of dust over the Sistan region and Hamoun Basin. Within this framework, satellite images from different years were used to identify changes in the lake's surface. Information about dust storm occurrence was obtained from Zabol meteorological station, 5 km from the Hamoun lakes (see Fig. 4). The ground-based measurements were primarily used to compare effects of the Hamoun surface on dust aerosols.

More specifically, the amount of dust loading during dust storms was measured using passive dust traps fixed at two monitoring towers (respectively, at four and eight meters above ground level in altitude), with one meter distance between the adjacent individual traps; the 4 m tower had four traps and the 8 m tower had 8 traps (Fig. 6). The two towers were established in open sites (station A and station B, denoted by red stars in Fig. 2 right panel) close to the dry-bed lake dust source region during the period August 2009 to July 2010. The dust sampler used in the campaign was developed by the Agricultural and Natural Research Center of Sistan (Fig. 6), and is a modified version of the SSDS sampler [66-67]. At the observation sites, the samplers collect airborne dust sediment. The traps were mounted on a stable bracket parallel to the wind direction. The samplers consist of a tube with a diameter of 12 cm. The sediment-laden air passes through a vertical 2.5 cm x 6 cm sampler opening in the middle. Inside the sampler, air speed is reduced and the particles settle in a collection pan at the bottom, while the air discharges through an outlet with a U shape. After each measurement, the samplers were evacuated to make them ready for measuring the following dust events. The collected samples were oven dried at 105 ^{o}C for 24 hours, and then, dried samples were weighed using an electronic scale in order to obtain total mass quantities at each sampling height and for each dust storm. The samples were also transported to a laboratory for chemical and mineralogical analysis.

Furthermore, soil samples were collected from topsoil (0–5 cm depth) at several locations in the dry-bed Hamoun lakes and downwind areas. These samples were analyzed to

investigate the chemical and mineralogical characteristics of dust, relevance of inferred sources and contributions to air pollution.

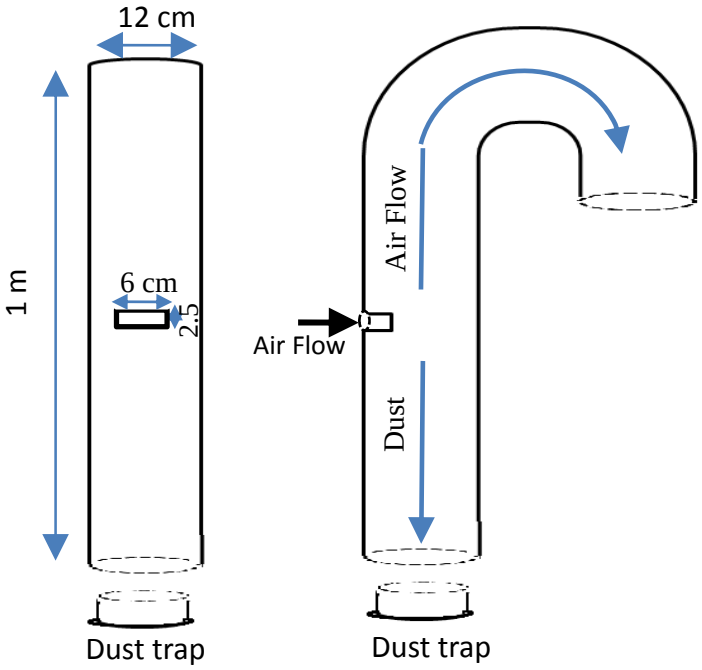

Figure 6. Schematic diagram of the dust sampler system.

These samples were analyzed for major and trace elements and for minerals by applying X-Ray Fluorescence (XRF) and X-Ray Diffraction (XRD) techniques, respectively. The samples were prepared for XRD analysis using a back loading preparation method. They were analyzed using a PANalytical X'Pert Pro powder diffractometer with X'Celerator detector and variable divergence and receiving slits with Fe filtered Co-Kα radiation. The phases were identified using X'Pert High score plus software. The relative phase amounts (weights %) were estimated using the Rietveld method (Autoquan Program). Mineral analysis by XRD is the single most important non-destructive technique for the characterization of minerals such as quartz, feldspars, calcite, dolomite, clay, silt and iron oxides in fine dust. Mineral phase analysis by XRD is one of the few techniques that are phase sensitive, rather than chemically sensitive, as is the case with XRF spectrometry. Quantitative mineralogical analyses using the XRD technique have been performed by a number of scientists over the globe [e.g., 68-70, 44, 71-72].

The sample preparation for XRF is made up of two methods, pressed powders and fusions. The former samples were prepared for trace element analyses and the latter for major

element analyses. Each milled sample (<75μm) was combined with a polyvinyl alcohol, transferred into an aluminum cup and manually pressed to ten tons. The pressed powders were dried at 100°C for at least 30 minutes and stored in a desiccator before analyses were conducted. For the fusion method, each milled sample (<75μm) was weighed out in a 1/6 sample to flux (Lithium tetraborate) ratio. These samples were then transferred into mouldable Pt/Au crucibles and fused at 1050°C in a muffle furnace. Aluminum cooling caps were treated with an iodine-ethanol mixture (releasing agent) and placed on top of the crucibles as they cooled. Some samples needed to be treated with an extra 3g of flux if they continued to crack. Finally, all geochemical samples were analyzed using the Thermo Fisher ARL 9400 XP+ Sequential XRF. The Quantas software package was used for the major element analyses and the WinXRF software package was used for the trace element analyses. The concentrations of the major elements are reported as oxides in weight percentages, while the trace element concentrations are reported as elements in parts per million (ppm).

Furthermore, in order to provide analysis of the air quality, PM_{10} concentration measurements were obtained by using an automatic Met One BAM 1020 beta gauge monitor (Met One, Inc.,) over Zabol. The instrument measures PM_{10} concentrations (in $\mu g.m^{-3}$) with a temporal resolution of one hour. The measurements were carried out at the Environmental Institute of Sistan located at the outskirts of Zabol during the period September 2010 to September 2011 (total of 373 days). The recording station is close to the Hamoun basin and is placed in the main pathway of the dust storms of the Sistan region. The hourly measured PM_{10} data were daily-averaged, from which the monthly values and seasonal variations were obtained. For further assessing the air quality over Zabol, the PM_{10} concentrations were used to calculate an Air Quality Index (AQI) [52].

6. Meteorology and climatology over Sistan

The climate over Sistan is arid, with low annual average precipitation of ~55 mm occurring mainly in the winter (December to February) and evaporation exceeding ~4000 $mmyear^{-1}$ [58]. During summer, the area is under the influence of a low pressure system attributed to the Indian thermal low that extends further to the west as a consequence of the south Asian monsoon system. These low pressure conditions are the trigger for the development of the Levar northerly wind, commonly known as the "120-day wind" [73], causing frequent dust and sand storms, especially during summer (June to August) [74, 56] and contributing to the deterioration of air quality [52]. Therefore, one of the main factors affecting the weather conditions over the region is the strong winds rendering Sistan as one of the windiest deserts in the world. These winds blow continuously in spring and summer (from May to September), and on some days during winter, and have significant impacts on the landscape and the lives of the local inhabitants.

The annual variation of mean Temperature (T), Relative Humidity (RH) and atmospheric Pressure (P) over Zabol (a large city in the Sistan region) during the period 1963 to 2010 is shown in Fig 7. The monthly mean T exhibits a clear annual pattern with low values in the

winter (9 to 12 °C) and high (~35 °C) in summer, following the common pattern found in the northern Mid-latitudes. During the summer period the maximum T often goes up to 46 or 48 °C causing an extremely large diurnal variation, which is a characteristic of many arid environments. RH illustrates an inverse annual variation with larger values in winter (50 to 57%) and very low values in summer (~25%), which are about 10 to 15% during daytime. During the period October to April P values are generally high (1020 to 1024 hPa in winter), which is above the standard mean sea level value of 1013.25 hPa. P values decrease during summer (~ 996 hPa in July) as a result of the Indian thermal low that develops over the entire south Asia during summer monsoon months. This has a direct impact on the intensity of the winds over the region, which has a monthly mean of as high as 12 $m.s^{-1}$ during June and July with frequent gusts of above 20 to 25 $m.s^{-1}$. In contrast, during late autumn and winter months the wind speed is confined to ~3 to 4 $m.s^{-1}$ [12].

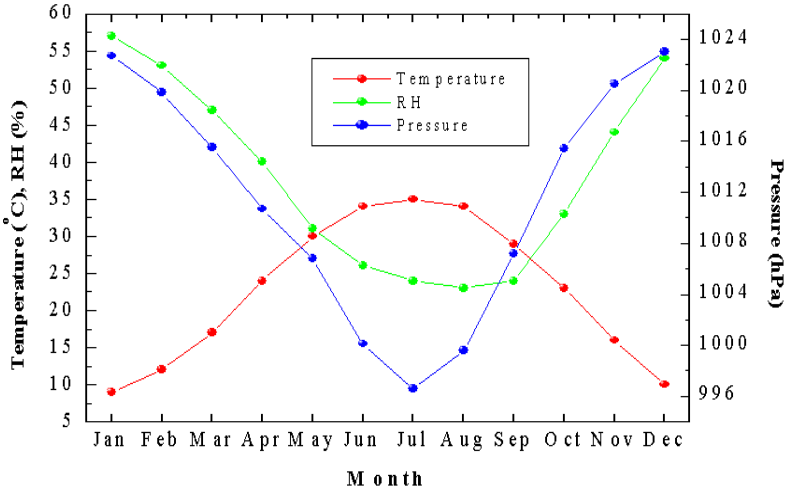

Figure 7. Monthly mean variation of air Temperature, Relative Humidity and atmospheric pressure in Zabol during the period 1963 –2010.

7. Temporal changes of Hamoun dry lake beds and dust storms

The dust storms over a region cause several climatic implications, environmental and human concerns [16, 75,18, 76, 36] and can be examined via multiple instrumentation and techniques. Among others, the analysis of the visibility records can constitute a powerful tool for monitoring of the seasonal and inter-annual variation of the dust storms, since the main result of such phenomena is the limitation of visibility and deterioration of air quality. The annual variation of visibility (as the main indicator for the dust storms) over Sistan follows a clear annual pattern, with large values in winter, usually above 10 km, and very low in summer (< 4 km on average) as analyzed from meteorological observations taken at Zabol (Fig. 8). A power-decreasing curve relation associated with 93% of the variance was observed between wind speed and visibility [12]. This inverse relation indicates that the wind speed does not act

as a ventilation phenomenon over Zabol, as usually occurs in coastal urban environments with local sea-breeze cells [77], but rather as a factor responsible for the deterioration of visibility, since the intense Levar winds are the cause of the dust outbreaks over Sistan. Therefore, the major dust storms over the region are associated with intense winds of northwesterly direction that are responsible for the deterioration of visibility to lower than 100 m in many cases.

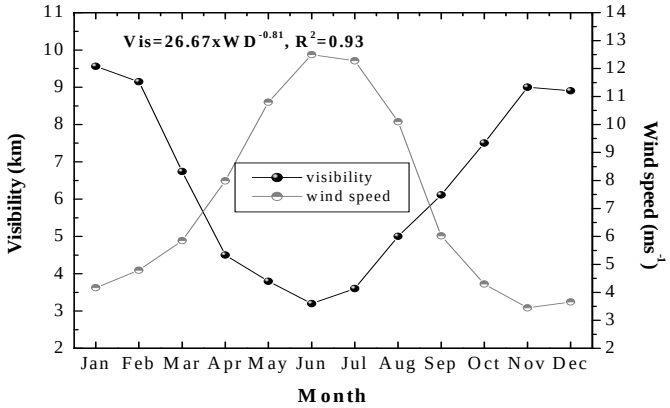

Figure 8. Monthly mean variation of the visibility (km) and wind speed (ms^{-1}) in Zabol during the period 1963–2009.

Although the visibility exhibits a clear annual pattern (Fig. 8) suggesting that the summer season is the favourable period for the occurrence of frequent and intense dust storms, long-term data series over Zabol (1963-2009) show that it contains considerable year-to-year variations (Fig. 9b). Focusing on recent years, the days with visibility <= 2 km have been dramatically increased from about 20 during 1995 to 1999 to >100 during 2000 to 2001. This is attributed to a severe drought period that dried the largest part of the Hamoun wetlands (see Fig. 5) and favored the alluvial uplift, as well as the frequency and mass intensity of dust storms that affected the visibility over Sistan (Fig. 9b). However, in the 2000s the days with very low visibility seem to have a decreasing trend, but remaining above the standards of the climatological mean. It is, therefore, concluded that the regional and synoptic meteorology (mainly precipitation) is strongly linked to land use – land cover changes over Hamoun and then, to dust outbreaks over Sistan region.

In contrast, the annual variation of the wind speed (Fig. 9a) exhibits an opposite pattern with higher intensities during summer (June and July) and lower in winter. As far as the wind direction is concerned, it is found from the Zabol data series that the northwestern direction clearly dominates, being more apparent in summer, while high percentages for intense winds are also associated with a northwesterly flow (Fig. 9a). The probability for intense winds to blow from other directions is low; summer winds are much more intense with ~27% of wind speeds above 11 ms^{-1}, while calm conditions are limited to 3% against 19% and 20% for autumn and winter, respectively. The higher frequency and intensity of northwestern winds is the reason for the frequent dust storms that affect Zabol. It is to be

noted that Zabol is located at the downwind direction of dust storms that normally originate from Hamoun (Fig. 2).

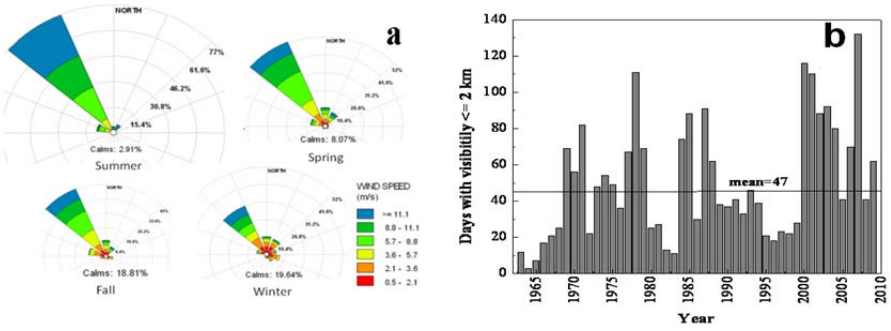

Figure 9. Flow chart of the seasonal wind speed and direction in Zabol during the period 1963-2010. The percentage of calm periods is shown at the bottom of each wind rose. The thickest bar represents wind speeds in excess of 12 m/s); (b) year-to-year variation of the visibility recordings at Zabol meteoroological station.

The water levels in the Hamoun lakes change considerably from year to year as has been discussed above. Table 1 summarizes the percentage of water surface in July in the Hamoun lakes, as well as the annual precipitation and number of dusty days during the period 1985-2005. Yearly variations of Hamoun lakes water surface identified four periods from 1985 to 2005: [10]:

1. A low-water period from 1985-1988: the Hamoun dried out or shrunk to a very small size almost every year, but there was some inflow every year.
2. A high-water period from 1989-1993: there was considerable inflow for five years, during which time the Hamoun only shrunk below the previous period's maximum levels for a very short time.
3. A medium-water period from 1994-1999: a dynamic balance of inflow and outflow maintained a reasonably high minimum water volume every year.
4. A dry period from 2000-present: the inflow ceased and a catastrophic drought ensued except for a flood in 2005 that immediately dried up before 2006.

On the other hand, Table 2 summarizes the correlation coefficients between the percentage of dried beds in July, precipitation and number of dusty days, i.e. the parameters that are included in Table 1. The analysis shows that precipitation has a direct effect on water levels (r=0.63 for Hamoun Saberi). On the other hand, in years with high precipitation the lakes had high water surface. Hamoun Saberi is also affected by the Farah river that has a closer watershed, but this correlation is low for both Hamoun Hirmand and Hamoun Puzak (r= 0.35 and r=0.54 respectively). The correlation between dusty days and percentage of dried Hamoun beds (100-percent of water surface) shows high correlation coefficient values regarding Hamoun Saberi and Baringak (r=0.88 and r=0.82 respectively) and lower correlation for Hamoun Hirmand (r= 0.63). The high correlation for the Hamoun Saberi and Baringak indicates that Sistan dust storms are directly affected by the north and

northwestern winds flowing through the Saberi. The year-to-year variation of the dusty days and the percentage (%) of dried bed lakes in Baringak and Hamoun Saberi (Fig. 10) indicates a co-variation of the examined parameters, thus suggesting that the land use – land cover changes play a major role in the occurrence of dust storms over Sistan region.

Year	Baringak	Saberi	Hirmand	Puzak	precipitation	Dusty days
1985	0	30	7	35	25.6	88
1986	35	65	12	53	72.8	30
1987	25	40	2	53	8.7	91
1988	15	50	6	50	69.5	62
1989	90	92	60	54	26.1	38
1990	90	98	70	72	96.1	37
1991	80	95	90	80	85.8	41
1992	80	98	80	93	80.9	33
1993	75	95	70	60	52.4	46
1994	43	60	20	60	116.6	39
1995	48	66	7	62	76.2	21
1996	62	90	47	70	84.3	18
1997	60	85	25	60	76.4	23
1998	80	100	73	60	61.4	22
1999	72	90	25	60	87.7	28
2000	0	12	0	0	26.8	116
2001	0	0	0	0	7.2	110
2002	0	5	0	0	37.5	88
2003	0	0	0	0	32.3	92
2004	0	0	0	0	51.1	80
2005	80	90	18	32	129.5	41

Table 1. Yearly variability of percentage of water surface in Hamoun lakes in July, annual precipitation and the dusty days (visibility <= 2km) over Sistan region

	Baringak	Hamoun Saberi	Hamoun Hirmand	Hamoun Puzak	Precipitation	Dusty days
Baringak	1					
Hamoun Saberi	0.96**	1				
Hamoun Hirmand	0.84**	0.80**	1			
Hamoun Puzak	0.80**	0.89**	0.74**	1		
Precipitation	-0.59**	-0.63**	-0.35	-0.54	1	
Dusty days	0.82**	0.88**	0.60**	0.81**	-0.730**	1

** Correlation is significant at the 0.01 level

Table 2. Correlations between percent of Hamoun dried beds in July and dusty days (1985-2005).

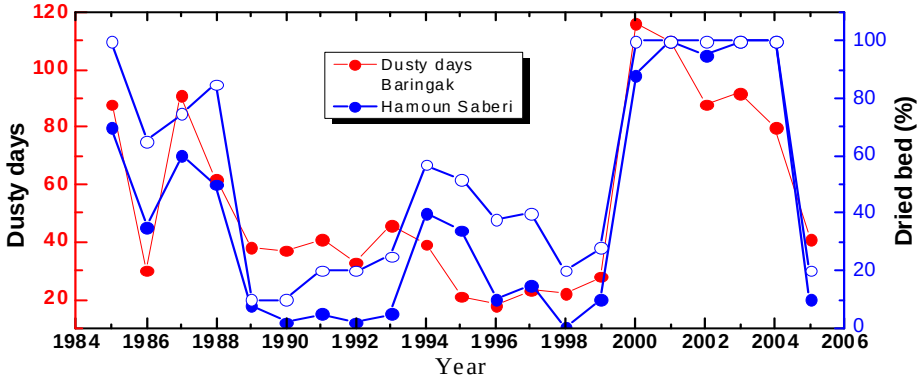

Figure 10. Yearly variability of the dusty days (visibility <= 2km) over Sistan region with association to percentage of Hamoun dried beds (1985-2005). The lower coverage of the Hamoun Basin by water (high percentage of dried beds) corresponds to higher number of dusty days over Sistan region.

8. Dust loading measurements

Dust activity is a function of several parameters, such as topography, rainfall, soil moisture, surface winds, regional meteorology, boundary layer height and convective activity [78-79.

Data on dust loading are available at only a few places around the world [e.g.80-84] and those presented here are the first for the Sistan region. Hence, obtaining measurements of horizontal dust flux will significantly increase our understanding of wind erosion and dust influences. Apart from the natural emissions of dust, [85] identified two ways in which human activities can influence dust emissions: (a) by changes in land use, which alter the potential for dust emission, and (b) by perturbing local climate that, in turn, alter dust emissions. As has been discussed above, both ways are considerably active over the Sistan region and Hamoun Basin.

The dust loading measured at the two stations close to the Hamoun basin for several dust events during the period August 2009 to July 2010 is plotted in Fig. 11. In the same graph, meteorological data from the Zabol station that give information about the duration of dust events (for the examined days as well as on the preceding or succeeding days, i.e. about 2-3 days before the peak-day of the dust storm) and daily mean and maximum wind speeds, are also plotted. The results of the average dust loading measured at eight heights at station B and at four heights at station A reveal considerable variation, ranging from ~0.10 to ~2.5 kgm^{-2}. In general, the highest dust loading is observed for dust events occurring in summer, but intense dust storms can also take place in winter, since the Hamoun basin is an active dust source region throughout the year. The dust loading is highly correlated with the duration of the dust storms, as shown from their correlation, with the linear regressions being statistically significant at the 0.99% confidence level (Fig. 12). Apart from the strong linkage to the duration of dust storms, the dust loading at both stations also seems to have a dependence on the daily mean and maximum wind speeds (not presented). However, this

dependence was found to be more intense and statistically significant (at the 95% confidence level) at station B, which is located closer to the dust source, whereas for station A the correlation was not found to be statistically significant. This finding emphasizes the strong effect of the wind speed on dust erosion and transportation, as well as on dust loading, at least for areas close to dust sources. However, the results show that the main factor that controls the dust loading at both stations is the duration of the dust storms, and secondly the wind speed. The role of the wind might have been found to be more critical if measurements were taken at the sampler stations instead of using the meteorological data from Zabol. The analysis showed that the total dust loading for the 19 events of measurements at station A is 16.9 kg m^{-2} corresponding to 0.88 kg m^{-2} per event, whereas at station B the measurements yielded 15.8 kg m^{-2} (17 events), corresponding to 0.93 kg m^{-2} per event. The larger dust loading at station B is attributed to the smaller distance from the source region.

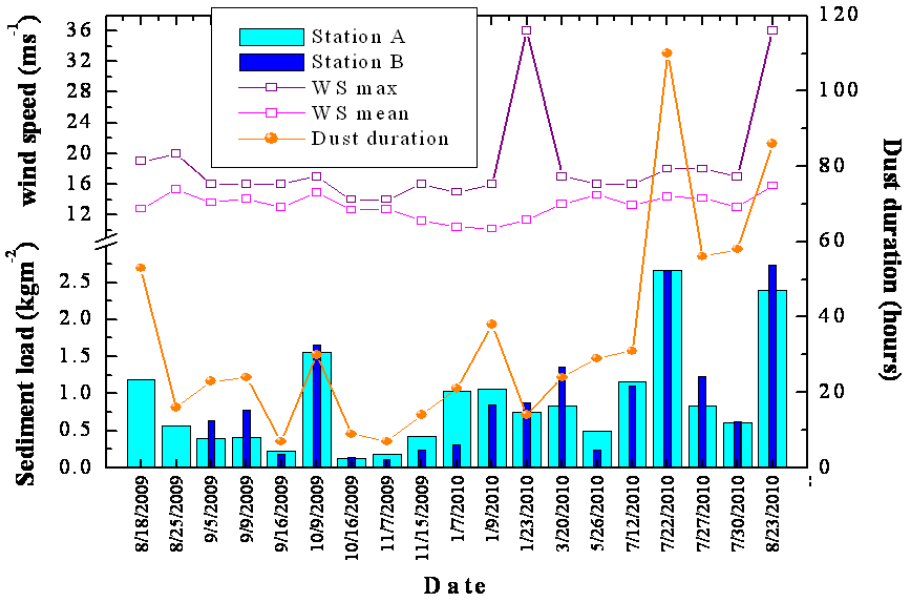

Figure 11. Average dust loading (kgm^{-2}) during various dust events in the Sistan region as measured at the 4m (station A) and 8m (station B) monitoring towers. The duration of dust events (hours), as well as the mean and maximum wind speeds on the dusty days were obtained from the Zabol meteorological station.

Figure 13 illustrates the height variation in dust loading during the dust storms measured at station A (19 days, up to 4m in height) and station B (17 days, up to 8m in height). Contrasting height variations measured during intense dust storms occurred between the two stations, while similar variations correspond to moderate and low dust storm events. More specifically, the dust loading shows an increase (decrease) with height in station A (station B), revealing a difference in the dust transport mechanisms. This finding can be explained by considering the fact that station B is located closer to the Hamoun dust source

region, meaning that uplift and newly transported dust concentration is higher near the surface. On the other hand, at station A that is located about 20 km away, the dust loading presents larger values up to 3 m since the near-ground dust particles have already been deposited near the source, and as the distance increases so does the dust-plume height. The diurnal variability of the dust loading at the two stations (not presented) showed increased mass concentrations during daytime that can be explained by enhanced convection and turbulent mixing in a deepened boundary layer. Furthermore, the local winds are stronger during daytime due to thermal convections.

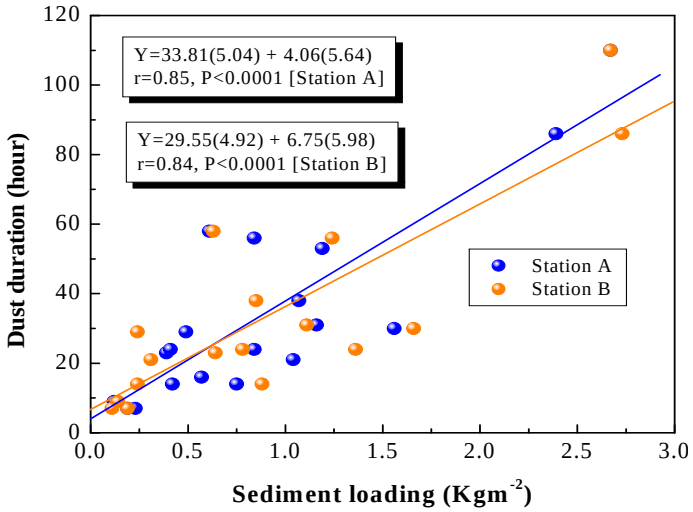

Figure 12. Correlation between dust loading measurements and duration of dust storm events for 19 days at station A and 17 days at station B.

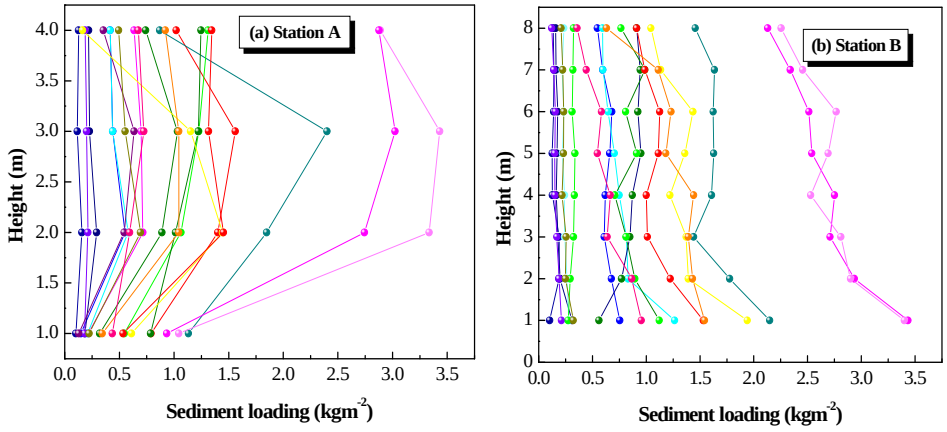

Figure 13. Height variation of the dust loading at stations A (a) and at station B (b) for several dust storm days. Green colors are loadings for winter, yellow for spring, red for summer and blue for autumn.

9. PM_{10} measurements

In order to provide a first ever in-situ analysis of the air quality over Sistan, PM_{10} concentration measurements were obtained by using an automatic Met One BAM 1020 beta gauge monitor (Met One, Inc.,) at Zabol [12]. The instrument measures PM_{10} concentrations (in $\mu g.m^{-3}$) with a temporal resolution of one hour. The measurements were carried out at the Environmental Institute in Sistan located at the outskirts of Zabol during the period September 2010 to August 2011. The recording station is close to the Hamoun basin and is placed in the main pathway of the dust storms in the Sistan region. The hourly measured PM_{10} data were daily-averaged, from which the monthly values and seasonal variations were obtained (Table 3). For further assessing the air quality over Zabol, the PM_{10} concentrations were used to calculate the Air Quality Index (AQI).

	Monthly Mean	Daily minimum	Daily maximum
	PM10 (μg.m-3)	PM10 (μg.m-3)	PM10 (μg.m-3)
January	196	29	597
February	147	13	787
March	262	21	2698
April	224	97	515
May	322	71	1276
June	627	100	1875
July	847	110	2007
August	807	155	2448
September	564	88	1046
October	531	100	2339
November	200	66	737
December	476	84	3094
Winter	273	13	3094
Spring	270	21	2698
Summer	716	100	2448
Autumn	484	66	2339

Table 3. Monthly mean, daily maximum and daily minimum PM_{10} concentrations in Zabol during the period September 2010 to August 2011.

The results show extremely large PM_{10} concentrations at Zabol (see Fig. 14). Even the mean values are much higher than the most risky and dangerous maximum levels provided by the U.S. Environmental Protection Agency (397 $\mu g.m^{-3}$). Throughout the year, and especially during the period June to October, the area suffers from severe pollution since even the lower PM_{10} values are above 100 $\mu g.m^{-3}$, while the maximum ones are usually above 1000 $\mu g.m^{-3}$. On the other hand, extreme PM_{10} measurements associated with severe dust events may also occur in other months, for example like December. Daily PM_{10} concentrations during major dust storms are about 10 to 20 times above the standard levels. Regarding the monthly mean PM_{10} concentrations, the results show extremely large values (>500 $\mu g.m^{-3}$) during the period June to October, reaching up to 847 $\mu g.m^{-3}$ in July.

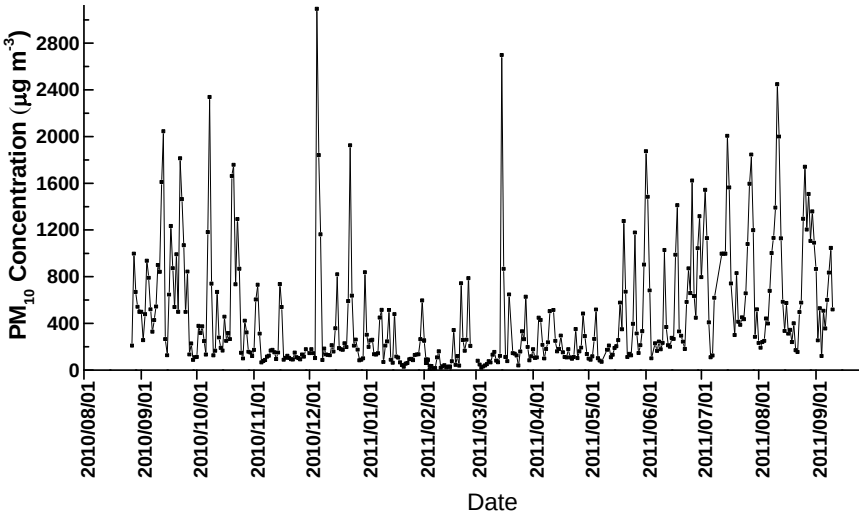

Figure 14. Daily PM_{10} concentrations at Zabol during the period 28/8/2010 to 10/9/2011.

The frequency of occurrence of PM_{10} concentrations for each season over Zabol is depicted in Fig. 15. In summer ~60% of the PM_{10} values were higher than 425 $\mu g.m^{-3}$, while the lower PM_{10} values occur in winter and spring with larger frequency in the 55-154 $\mu g.m^{-3}$ interval. A very significant finding is the very low frequency for PM_{10} concentrations below ~400 $\mu g.m^{-3}$ in summer, suggesting an extremely turbid atmosphere with frequent dust storms and near absence of clear or relatively clear conditions over Sistan during summer. Autumn also presents high frequency in the >425 $\mu g.m^{-3}$ interval that might be due to continuation of the Levar winds in September favouring the dust storms over Sistan.

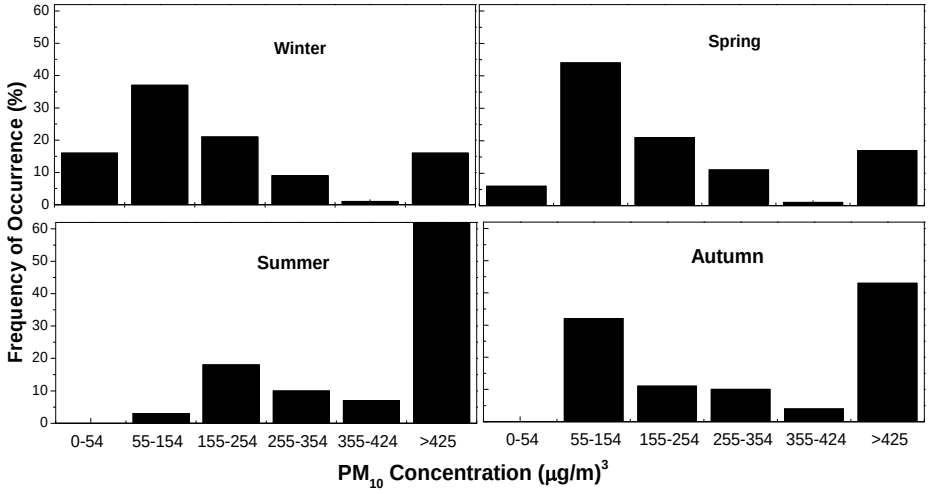

Figure 15. Frequency (%) distribution of the daily PM_{10} values for each season in Zabol.

10. Air quality index (AQI)

In order to identify the impact of air pollution on human health, air pollution indices are commonly used, of which the AQI is the most well known [86-88]. As a consequence, the AQI is a powerful prenatainarry tool to ensure public health protection [86].

The AQI is divided into six categories, varying from 0 to 500, with different health impacts [86] as listed in Table 4. The two first AQI categories (good and moderate, <155 PM_{10} $\mu g.m^{-3}$) have no impact on health, while the last AQI category (hazardous, >424 PM_{10} $\mu g.m^{-3}$) is associated with a serious risk of respiratory symptoms and aggravation of lung disease, such as asthma, for sensitive groups and with respiratory effects likely in the general population [89, 87]. The AQI for Zabol was calculated for the period September 2010 to July 2011.

Health Quality	AQI	PM10 (μg.m-3)	Days	(%)
Good	0-50	0-54	21	5.7
Moderate	51-100	55-154	106	28.6
Unhealthy for sensitive people	101-150	155-254	66	17.8
Unhealthy	151-200	254-354	36	9.7
Very unhealthy	201-300	355-424	12	3.2
Hazardous	301-500	425<	129	34.9

Table 4. Health quality as determined by the Air Quality Index (AQI), PM_{10} and number of days with severe pollution in Zabol during the period September 2010 to July 2011.

Based on the technological rules related to AQI, the following formula was used to derive the PM_{10} concentration from AQI [90, 88]:

$$I = \frac{I_{high} - I_{low}}{C_{high} - C_{low}}(C - C_{low}) + I_{low}$$

Where I is the concentration of PM_{10}, I_{low} and I_{high} are AQI grading limited values that are lower and larger than I (AQI index), respectively, and C_{high} and C_{low} denote the PM_{10} concentrations corresponding to I_{high} and I_{low}, respectively.

Provisional studies focusing on air quality and dust over Iran have already been carried out. For example, amongst others, [91] performed a comparative study of air quality in Tehran during the period 1997 to 1998. The results revealed that in 1997 the air quality on 32% of the days was unhealthy, and on 5% of the days it could be regarded as very unhealthy, whereas in 1998 the unhealthy and very unhealthy days increased to 34% and 6%, respectively. [92] studied the air quality in Tehran and Isfahan and offered solutions for its improvement using the AQI. It was found that on 329 days of the year in Tehran, and on 34 of the days in Isfahan, the AQI departed beyond 100. [93] also studied AQI in Tehran

reporting that on 273 days in 2001 the values were higher than those set for the air quality standards; 13% of the days were considered as very unhealthy and 0.27% were classified as dangerous. [52] found that 15 % of the days were unhealthy for sensitive people in the city of Zahedan thatwas affected by Sistan dust storms, while 2 % were associated with a high health risk or were even hazardous.

Comparing the present results with those of the above-mentioned studies, it is concluded that the Sistan region experiences much higher PM concentration levels. Assessment of air quality in Zabol shows that 243 days out of 370 (65%) exhibit air pollution levels of above the air quality standards (>155 $\mu g.m^{-3}$), a fraction that is much higher than that (26.5%) reported for Zahedan city located also in Sistan about 200 km south of Zabol [52]. The most significant finding is the 129 days (34.9%) that are characterized as hazardous (Table 4), which in combination with the adverse effects on human health, make it clear that environmental conditions in the Sistan region are rather poor for human well-being. On the other hand, only 5.7% of the days are associated with low pollution levels when the air quality is considered satisfactory and air pollution poses little or no risk. Several studies have shown that ambient air pollution is highly correlated with respiratory morbidity, mainly amongst children [94, 36, 95]. The results gathered from hospitals in the Sistan region showed that during dust storms respiratory patients increased significantly, especially those affected by chronic obstructive pulmonary disease and asthma. The percentage of these diseases increases in summer (June and July) [53]. Apart from the dust storms, re-suspended dust within the urban environment is a strong source of PM_{10} concentrations, while urban-anthropogenic and industrial activities are considered to have a much lower effect on the air pollution over Zabol.

The mean diurnal variation of PM_{10} concentrations for each season in Zabol indicates a clear pattern for all seasons except winter, with the maximum of the diurnal variation being observed in the middle of the day (~08:00-11 LST) while in winter PM_{10} values reach a maximum in the afternoon hours to early morning (~16:00 – 02:00 LST). In general, solar heating and vertical mixing of pollutants are the main factors for the reduction of PM_{10} levels at local noon to early afternoon hours. However, the maximum PM_{10} concentrations normally occur between 08:00 and 11:00 (LST) over Sistan. The diurnal PM_{10} variability in all seasons, except winter, is closely associated with the intensity of the wind speed measured at the Zabol meteorological station (see Fig. 16). This wind, being northerly in direction, carries large quantities of dust from the Hamoun dry lake bed. The mean diurnal wind speed variation is similar for all seasons; however, the wind favors the increase of aerosol load in summer and autumn (maximum PM_{10} for higher wind speeds). Note that the Hirmand River and some other ephemeral channels provide little water in winter and spring to the Hamoun lake beds. Therefore, in early summer, the Hamoun lakes are wet and at the end of summer and early autumn are always completely dried out. On the other hand, the Levar winds continue also in September and so high wind speeds cause huge dust storms.

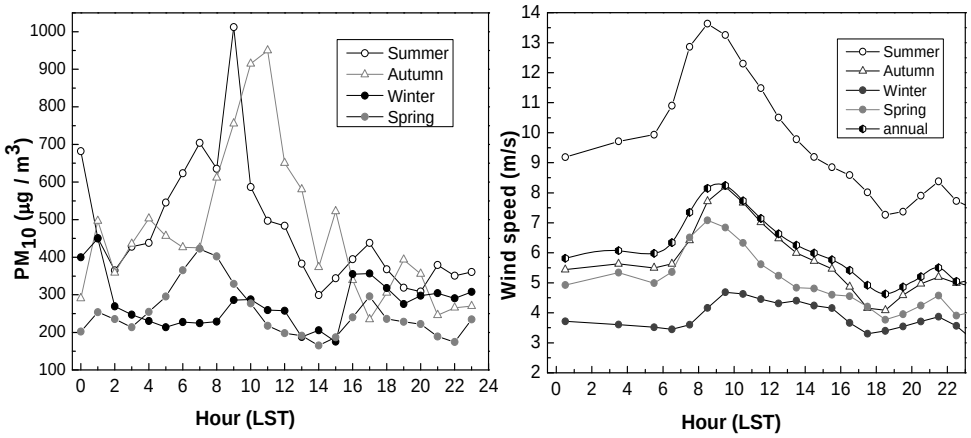

Figure 16. Mean hourly variation of the PM_{10} (left panel) and wind speed (right panel) for each season in Zabol.

11. Mineralogical characteristics of dust

In order to understand the influence of dust on the atmospheric environment, climatic system and health and to establish effective remedial policies and strategies, it is regarded as necessary to investigate the compositional (chemical and mineralogy) characteristics of airborne and soil dust over Sistan. To the best of our knowledge there are currently no published studies about the geochemical characteristics and dust mineralogy in this region. Moreover, nearby locations, Bagram and Khowst in Afghanistan, were selected for analyzing the mineralogical dust composition, major and trace elements within the framework of the Enhanced Particulate Matter Surveillance Program (EPMSP) campaign [44]. Furthermore, mineralogical and geochemical characteristics of dust were recently examined at Khuzestan province in southwestern Iran [72].

In this Chapter, an overview of the geological-geochemical characteristics of airborne and soil dust in the Sistan region is given for airborne and soil samples collected during the period August 2009 to August 2010. The chemical constituents during major dust storms over the region are analyzed at two locations (Fig. 2), also investigating the relationship between the chemical constituents of the dust storms and those of the inferred (Hamoun) source soils. The mineralogy percentage composition averaged at all heights for each day is shown in Fig. 17a, b for stations A and B, respectively. The chemical formulas of the main mineralogical components are given in [96], as well as the chemical reactions of dust with atmospheric constituents and trace gases during the dust life cycle. The mineralogical composition corresponds to screened samples with diameter <75 μm and can constitute an indication of both regional geology and wind transported dust that is deposited in local soils [44].

Emphasizing the dust mineralogy at station A, it is seen that the airborne dust is mainly composed of quartz, which is the dominant component (26-40%) for all the days of observations. Calcareous particles, mainly consisting of calcite, are the second dominant

mineralogical component over the site with average mass percentage of 22%, while micas (muscovite) contribute 13% and plagioclase (albite), 11%. The remaining components contribute much less to the dust mass, while chlorite (6.3%) is apparent in all dust samples for all days. The others, i.e. dolomite, enstatite, gypsum, halite, etc are present only in some samples with various percentages. It is quite interesting to note that quartz is much more common over Sistan than the feldspars (plagioclase, microcline and orthoclase).

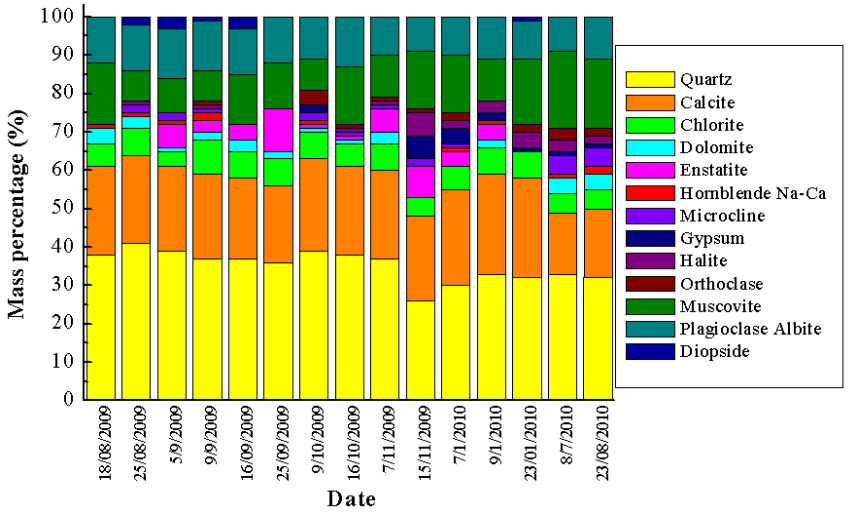

(a)

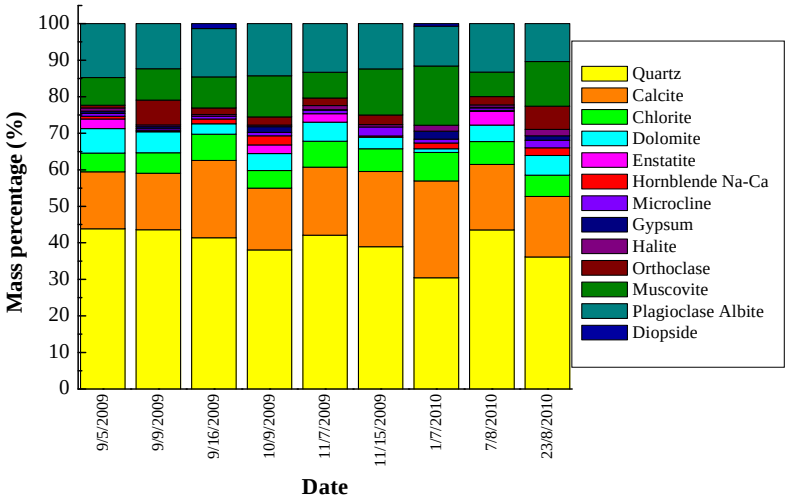

(b)

Figure 17. a. Mineralogical composition as obtained from XRD analysis for airborne dust samples collected on different days in station A. **b.** Same as in Figure 17a, but for the station B.

The mineralogical analysis for the 9-days recorded data at station B (Fig. 16b) shows more or less similar results to those obtained for station A and, therefore, any discussion will be given on their comparison (Fig. 19). The mineralogical composition has the same descending order as in station A, i.e. quartz (39.8±4.4%), calcite (18.8±3.5%), plagioclase (albite) (12.7±1.4%) and muscovite (10.1±3.2%). On the other hand, dust deposition may influence biogeochemical cycling in terrestrial ecosystems, while dust accumulation in soils can influence texture, element composition and acid neutralizing capacity [97-98]. Furthermore, the chemical and mineralogical composition of soil dust provides useful information about its provenance [99], radiative forcing implications [100] and human health effects [101]. For these reasons, in addition to the airborne dust samples, soil samples were collected at 16 locations around Sistan and Hamoun, at depths ranging from 0 to 5 cm from the soil crust. The results of soil sample mineralogy are summarized in Fig. 18. From an initial consideration of these results, it is established that the soil samples exhibit similar mineralogy to the airborne dust at both stations, thus suggesting similarity in sources for both airborne and soil dust. On the other hand, some soils in the Sistan region have been primarily formed from dust transported from the Hamoun lakes, presenting large similarities in mineralogy and chemical composition to airborne dust. However, atmospheric chemical reactions involving dust and aerosols of other types can alter the chemical characteristics of dust before its deposition [102]. Therefore, the mineralogy of the soil samples may differ significantly in comparison to the results obtained for airborne dust at stations A and B, since some of the soil samples (11 samples) were collected in the Hamoun dried lakes and others (five samples) around stations A and B.

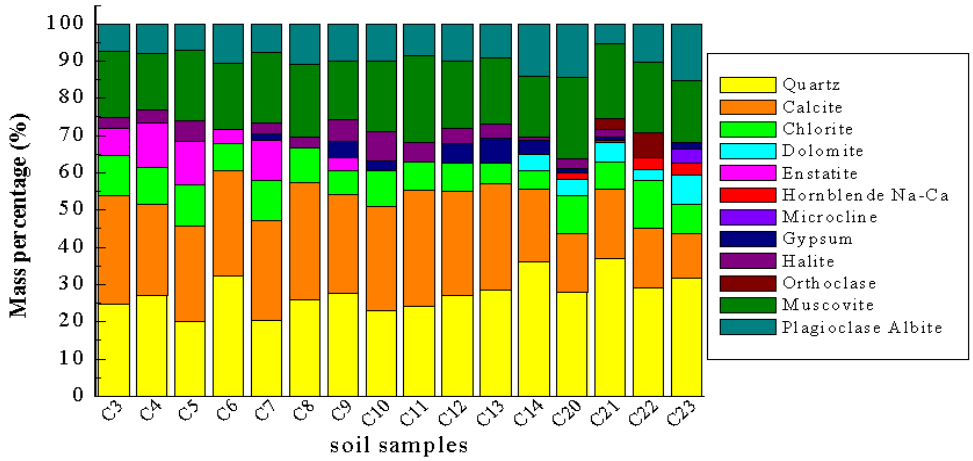

Figure 18. Mineralogical composition as obtained from XRD analysis for soil samples collected at various locations in the Hamoun Basin.

Figure 19 summarizes the results from the mineralogical analysis of samples taken at the two stations and from the soil samples, allowing a quantitative comparison between them. The vertical bars correspond to one standard deviation from the mean for both airborne and

soil samples. The distance from the source region from whence dust is deposited also influences the particle size distribution, mineralogy and chemical composition of dust. Therefore, generally speaking, at local scales quartz clearly dominates with fractions up to ~50%, while as the distance from the dust source increases, feldspars (plagioclase, microcline) and phyllosilicate minerals (illite and kaolinite) present increased fractions [103, 42]. However, in our study the dust samples were all obtained within the same area and, therefore, are mineralogically similar. Nevertheless, station B, which is located closer to the Hamoun basin, the source of dust exposures, exhibits higher percentages of quartz, while station A (near to Zabol city) exhibits higher concentrations of calcite and muscovite compared to station B. On the other hand, the soil samples exhibit a lower mean percentage for quartz (27.7±4.7) and higher percentages for calcite, chlorite, halite and muscovite compared to the airborne samples.

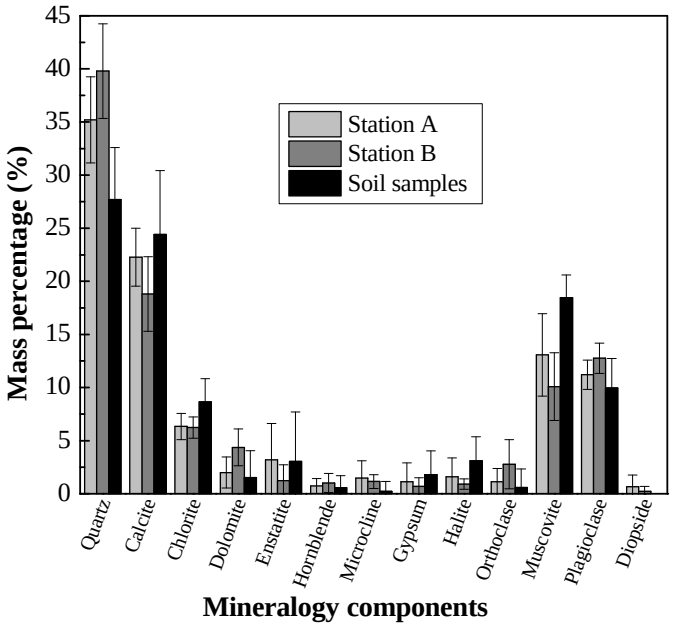

Figure 19. Average mineralogy components for airborne dust samples at stations A and B and for soil samples obtained at various locations in Hamoun Basin. The vertical bars express one standard deviation from the mean.

These mineralogical airborne dust and soil compositions, derived essentially from the Hamoun source region, reflect the composition of the material available from this provenance as well as the relevant grain size characteristics, enabling the wind storms to entrain this material into the lower atmosphere. While most of the minerals (quartz, feldspars of various types, muscovite) can easily be tied to basement-type lithology of generally gneissic-granitic character, others (chlorite, pyroxenes and hornblende) rather

suggest mafic parent rocks, as can be inferred from basic mineralogical analysis [e.g.,104] . However, the calcite, dolomite, halite and gypsum suggest evaporate minerals, although both calcite and dolomite can also reflect alteration products of primary acid or mafic rock constituents. The inferred evaporate minerals reflect local derivation of salt from desiccating water bodies in the Hamoun lakes, originally formed from altered transported components via the Hirmand river system. Thus, the semi-quantitative mineral determinations for the airborne dust over the Sistan region support derivation of the particles from well weathered and well eroded (transported) argillaceous alluvium from the extensive Hirmand river system draining Afghanistan and terminating in the Hamoun Basin. The general geology of Afghanistan encompasses extensive terrains of both acidic and mafic rocks, while similar mineralogical composition of dust (i.e. dominance of quartz, but lower percentage of calcite) was found at the Bagram and Khowst sites located in eastern Afghanistan [44]. More specifically, they found that these sites are underlain by loess (wind deposited silt), sand, clay and alluvium containing gravel. As shown in Fig. 2, as well as in other studies [44, 51, 12], nearly the whole of Afghanistan is affected by the dust storms originating from Hamoun, since the dust plume usually follows a counter-clockwise direction, carrying wind-blown dust towards eastern Afghanistan. Similarly to our findings, the airborne dust at selected locations in southwestern Iran was found to be composed mainly from quartz and calcite, suggesting detritus sedimentary origin, followed by kaolinite and a minor percentage of gypsum [72]. Furthermore, [44] found that airborne dust samples derived from poorly drained rivers and lakes in central and southern Iraq contain substantial calcite (33– 48%), quartz and feldspar with minor chlorite and clay minerals. Previous studies [105-106], have shown that silicate minerals (quartz, feldspars) and phyllosilicates (illite, kaolinite, smectite/montmorillonite clays, chlorite) dominate aeolian dust. Dust samples may also contain substantial amounts of carbonates, oxides, gypsum, halite and soluble salts, but the quantity and percentage of these minerals are quite variable from site to site.

12. Elemental composition of dust

Knowledge of the chemical composition of airborne dust is necessary for clarifying the likely source regions and is important for quantitative climate modelling, in understanding possible effects on human health, precipitation, ocean biogeochemistry and weathering phenomena [50]. Chemical analysis of dust provides valuable information about potentially harmful trace elements such as lead, arsenic and heavy metals (Co, Cr, Cu, Ni, Pb). On the other hand, the major-element and ion-chemistry analyses provide estimates of mineral components, which themselves may be hazardous to human health and ecosystems and which can act as carriers of other toxic substances. The chemical analysis of dust samples at both stations was performed via XRF analysis for the major oxides (Figs. 20a, b).

In general, the analysis reveals that all samples at both stations contain major amounts of SiO_2, mainly in the mineral quartz, variable amounts of CaO in the mineral calcite, plagioclase feldspar and to a limited extent in dolomite, as well as substantial Al_2O_3 concentrations. More specifically, average major elements of airborne dust at both stations indicate a predominant SiO_2 mass component (46.8 – 47.8%) with significant CaO (12-12.2%)

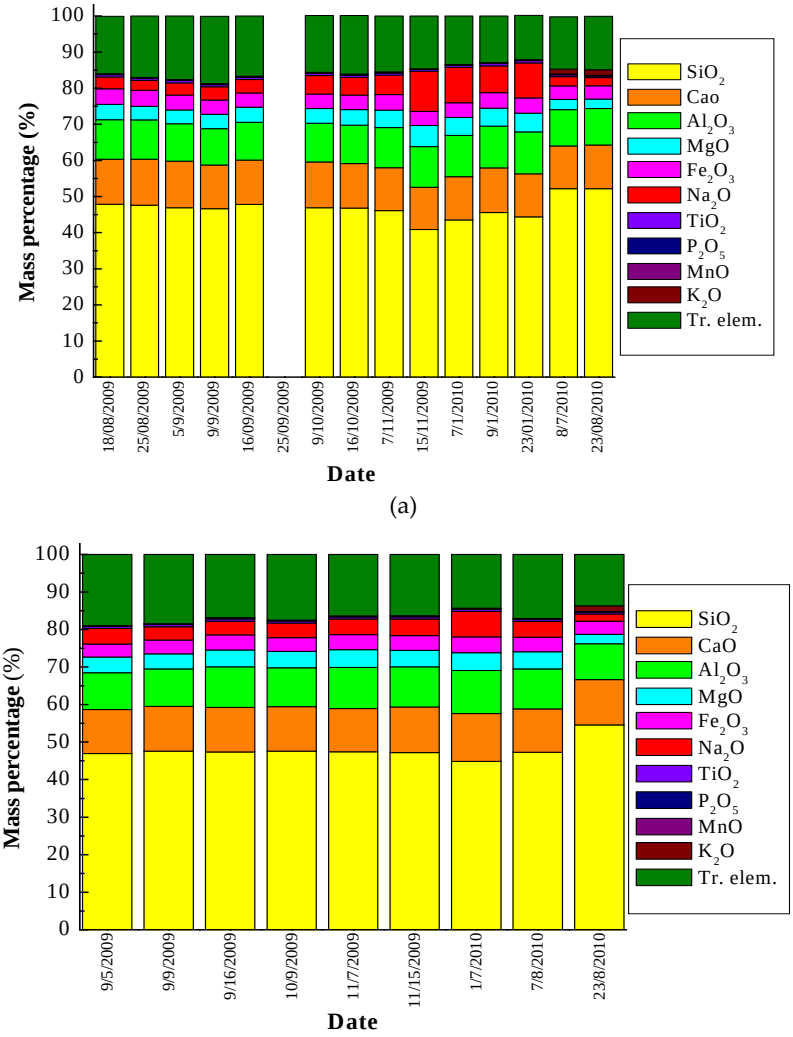

Figure 20. **a.** Major elements (oxides) for airborne dust samples obtained on different days at Station A analysed by means of XRF. **b.** Same as in Fig. 20a, but for the station B.

and Al_2O_3 (10.4-10.8%) contributions; a few percent of Na_2O (4.2-5.4%), MgO (4.3%) and total iron as Fe_2O_3 (3.8-4.1%), as well as trace amounts (<1%) of TiO_2, K_2O, P_2O_5 and MnO, while the remaining major elements (Cr_2O_3, NiO, V_2O_5, ZrO_2) were not detected by XRF analysis (Figs. 20a, b). When compared to various average shale analyses in the literature (Geosynclinal Average Shale and Platform Average Shale from [107] ; Average Shale from [108]; North American Shale Composite from [109], the Sistan dust is significantly depleted

in SiO_2, Al_2O_3, K_2O and total Fe and significantly enriched in CaO, Na_2O and MgO. The MgO is largely contained in dolomite and, to a lesser extent, in clay minerals such as palygorskite and montmorillonite [78, 44]. These components can be ascribed to the importance of evaporate minerals such as calcite, dolomite, halite and gypsum (as also suggested by the mineralogical analysis) inferred to have come from the desiccation taking place in the Hamoun dust source region. Furthermore, the elevated values for the trace elements Cl, F and S (Table 5) support the latter postulate as it would be expected from an evaporate-rich source for deflation of dust [e.g.,110]. Similar to the elemental composition of dust over Sistan, [44] determined a high fraction of SiO_2 in silt, less CaO in calcite and slightly more Al_2O_3 in clay minerals at the Khowst site. At both Afghanistan sites (Bagram and Khowst), the SiO_2 was dominant with fractions of about 50-55%, followed by Al_2O_3, CaO and MgO.

By comparing the major elements of different dust storms, some interesting relationships have been found. More specifically, on days (e.g. 15/11/2009, 7/1/2010, 23/1/2010) (Fig. 20a) when airborne dust was relatively depleted in SiO_2, enhanced MgO and, particularly, Na_2O values were recorded. Conversely, when SiO_2 values were higher (e.g. 8/7/2010, 23/8/2010), both MgO and Na_2O contributions dropped. This suggests that certain intense dust storms were richer in evaporate source material (i.e., elevated MgO and Na_2O) coming from Hamoun dried lake beds, while others had more silica, reflecting weathered rock detritus from the Hirmand river and Afghanistan mountains. An explanation of these variable chemical compositions of dust samples is a real challenge, but it is postulated here that they may reflect local desiccation cycles and, possibly, even micro-climatic changes in the Hamoun-lakes dust source region. Excessive desiccation of the lakes would enhance potential evaporate minerals for deflation in drier periods, while in wetter periods, airborne dust would logically have been derived more from weathered fluvial detritus rich in SiO_2.

Figure 21 summarizes the results of the elemental compositions determined by XRF analysis at both stations. For comparison reasons, the mean elemental composition found for several sites in southwestern Iran (Khuzestan province) [71-72] is also shown. The vertical bars express one standard deviation from the mean. Concerning the major elemental oxides over Sistan, both stations exhibit similar results, well within the standard deviations, suggesting that the transported dust over Sistan is locally or regionally produced with similarity in source region. In contrast, the mean elemental composition of airborne dust over Khuzestan province exhibits remarkable differences from that over Sistan, revealing various source regions and dust mineralogy. More specifically, the SiO_2 percentage is significantly lower and highly variable over Khuzestan, which is also characterized by higher contributions of Na_2O, MgO and K_2O compared to Sistan. The dust storms over southwestern Iran may originate from local sources as well as being transported over medium- and long-ranges from different sources located in Iraq as well as in the Arabian Peninsula. A comparative study of the mineralogy and elemental composition of airborne dust at several locations in Iraq, Kuwait and the Arabian Peninsula [44] has shown significantly variable contributions, suggesting differences in overall geology, lithology and mineralogy of these regions. In further contrast, airborne dust over Sistan seems to have its individual characteristics originating from local and well-defined sources.

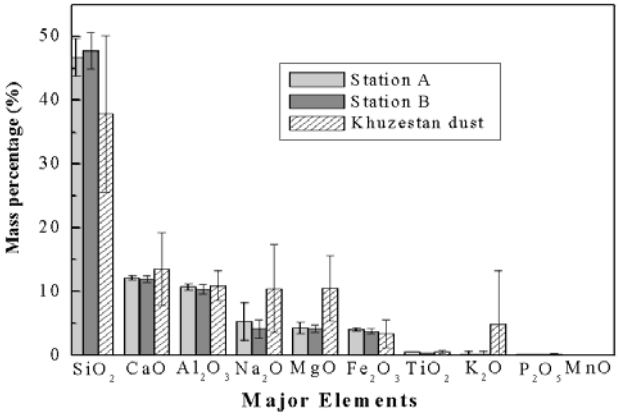

Figure 21. Average X-ray fluorescence (XRF) results for major dust elements in stations A and B. Similar results obtained in Khuzestan Province, southwestern Iran [71-72] are also shown for comparison reasons.

The Earth's crust is dominated by silicon and aluminum oxides. Numerous studies [78, 50 and references therein] reviewing the elemental composition of airborne dust over the globe report that mineral dust is composed of ~60% SiO_2 and 10-15% Al_2O_3. The contribution of other oxides, i.e. Fe_2O_3 (~7%), MgO (~2.5%) and CaO (~4%), are, in general, more variable depending on source location. Furthermore, the review study of [96] showed that airborne dust samples collected over the globe have fairly small variations in elemental composition. The CaO concentrations over Sistan are found to be much higher than those (5.5%) summarized in [96].

13. Trace elements

The average concentrations of trace elements (in ppm) in dust samples collected during major dust storms at stations A and B are summarized in Table 5, as obtained from XRF analysis. The results show that the dominant trace elements over Sistan are F and Cl, with the former being dominant in the vast majority of the dust events at station A. However, on two days (8/7/2010 and 23/8/2010) the Cl concentrations were extremely large, thus controlling the average value; there is a lack of observations at station B on 23/8/2010, thus the lower average Cl concentration. Note that on both these days, the SiO_2 component is large, while MgO and Na_2O are low (Fig. 20a). The dominance of chlorine indicates soil salinization in the Hamoun basin and along the Hirmand river and its tributaries. Furthermore, S exhibits higher concentration at station A, while for the other elements the concentrations between the two stations are more or less similar. The concentrations of potentially harmful and toxic elements, like Cs, Pb and As are, in general, low at both stations; however, Ba, Cr and Zn present moderate concentrations.

On the other hand, the analysis of the major element ratios provides essential knowledge of the dust chemical composition and source region. The ratios of Si/Al at stations A and B are

similar (7.8±0.8 and 8.3±0.9, respectively), due to the presence of silicate and aluminosilicate minerals in most dust samples. The ratios of Mg/Al (0.90±0.16, 0.92±0.12), Ca/Al (3.09±0.19, 3.12±0.19) and Fe/Al (0.51±0.02, 0.49±0.01) at the two stations suggest contributions of clays and Ca-rich (calcite) minerals to the chemical compositions of the airborne dust. In contrast, the Fe/Al ratio is low over Sistan and is nearly half of that found for airborne dust over southwestern Iran and several locations over the globe [72], but is comparable to that found over central Asia [111]. It should be noted that this ratio remains nearly invariant, ranging from 0.47 to 0.54, for all the collected dust samples at both stations and can be a good surrogate for the dust source region, since any variation in Fe/Al mainly corresponds to variations in clay minerals and not to coating during dust transportation [50]. In contrast, the Ca/Al ratio exhibits the highest variations from sample to sample (2.80-3.46), since it is influenced by particle size, with higher values as particle-size increases [72]. Synoptically, all the ratio values and the low standard deviations suggest similarity in geochemical characteristics over Sistan and a uniform source of airborne dust.

Trace Elements		
Parts per million (ppm)	Station A	Station B
Cl	28670	15047
F	13938	13456
S	4445	2506
Ba	210	253
Sr	154	125
Zr	83	76
Cr	70	84
V	69	69
Zn	57	51
La	30	32
Rb	24	19
Ni	18	16
Ce	17	16
Cs	14	13
Sc	11	11
Cu	11	11
Pb	10	10

Table 5. Average X-ray fluorescence (XRF) values for trace elements of airborne dust for stations A and B.

14. Conclusions

The present Chapter focused on shedding light on the dust loading, PM concentrations, physical and chemical composition of dust in the Sistan region, southeastern Iran, which constitutes a major dust source region in south west Asia. Sistan region is a closed topographic low basin surrounded by arid and rocky mountains, while its northern part

drains the Hilmand river, thus constituting a wetland area known as Hamoun. Hamoun lakes complex have an area about 4500 Km^2 with water volumes of 13025 million m^3 and play the role of a "water cooler" for the region when they are full of water as the severe winds blow across the lakes.

Severe droughts over the past decades, especially after 1999, have caused desiccation of the Hamoun lakes, leaving a fine layer of sediment that is easily lifted by the wind and therefore making the basin one of the most active sources of dust in south-west Asia [56, 50]. The strong "Levar", especially during the summer season, blows fine sands off the exposed lake bed and deposits this detritus within huge dune bed forms that may cover a hundred or more villages along the former lakeshore. As a consequence, the wildlife around the lake has been negatively impacted and fisheries have been brought to a halt, which also implies an impact on society. The drainage of the Hamoun wetlands, in association with the intense Levar winds in summer, is the main factor responsible for the frequent and massive dust storms over the Sistan region. Analysis of water surface in combination with dust storms showed that the Hamoun dried beds, particularly Hamoun Saberi and Baringak, have a dramatic effect on dust storms as sources of aerosols.

Systematic PM concentrations were measured in Zabol city, affected by the Sistan dust storms, covering the period September 2010 to August 2011. The results show that the PM_{10} concentrations were considerably higher than the corresponding European Union air quality annual standard. The analysis of the daily PM concentrations showed that the air quality is affected by dust storms from the Sistan desert, which may be very intense during summer. Hamoun, as an intense dust source region, caused a dramatic increase in PM_{10} concentrations and a deterioration of air quality (65% of the days were considered unhealthy for sensitive people and 34.9% as hazardous).

Dust loading from the Hamoun basin appears to have a significant contributing influence on the development of extreme dust storms, especially during the summer days. This influence firstly seems to depend on the intensity and duration of dust storms, and secondly, on the distance from the source region, the wind speed and altitude. The grain-size distribution of the dust loading was strongly influenced by the distance from the dust source, since grain sizes shifted to larger values towards station B that is closer to the Hamoun basin. Furthermore, the particle size distribution exhibited a shift towards lower values as the altitude increases, with this feature seen to be more obvious amongst larger size particles, while the frequency of particles below 2.5 μm seemed not to be affected by altitude. In general, the regional dust loading and characteristics are subject to significant spatio-temporal variability. This finding necessitates more systematic observations at as many locations as possible around the Hamoun basin in order to improve the understanding of forcing dynamics, transport mechanisms as well as to quantify the dust amounts emitted from the Hamoun basin.

To fully understand mineral dust characteristics and the potential impact on human health, dust mineralogy and geochemical properties were examined in the Sistan region by collecting airborne samples at two stations and soil samples from several locations over

Sistan and the Hamoun basin. The Sistan region is an ideal site to study the nature of dust storms as it receives large amounts of fine alluvial material from the extended Hirmand river system draining much of the Afghanistan highlands, which comprise crystalline basement rocks, Phanerozoic sediments and extensive flood basalts. As a result, large quantities of quartz-rich, feldspar- and mica-bearing silt, as well as mafic material from flood basalt sources and carbonate minerals from dolomites, are transported to the Hamoun wetlands in northern Sistan. Due to droughts at Hamoun and large irrigation projects upstream on the river catchment, extensive desiccation has occurred in the wetlands resulting in large dry lake environments. These have produced large quantities of evaporate minerals to add to the alluvial silts, and the combination of these materials provides the provenance for the airborne dust.

Dust aerosol characterization included chemical analysis of major and trace elements by XRF and mineral analysis by XRD. The results showed that quartz, calcite, muscovite, plagioclase and chlorite are the main mineralogical components of the dust, in descending order, over Sistan, and were present in all the selected airborne dust samples. In contrast, significantly lower percentages for enstatite, halite, dolomite, microcline, gypsum, diopside, orthoclase and hornblende were found, since these minerals occurred only in some of the samples at both stations. On the other hand, SiO_2, CaO, Al_2O_3, Na_2O, MgO and Fe_2O_3 were the major elements characterising the dust, while large amounts of F, Cl and S were also found as trace elements. The mineralogy and chemical composition of airborne dust at both stations were nearly the same and quite similar to the soil samples collected at several locations downwind. This suggests that the dust over Sistan is locally emitted, i.e. from the Hamoun basin, and in a few cases can also be long-range transported to distant regions. On the other hand, individual dust storms showed significant differences between either evaporite-dominated aerosols or those characterized by deflation from alluvial silts. These possibly reflect either localized climatic cyclicity or desiccation cycles. However, in some cases the soil samples showed poor comparisons with aerosol compositions, suggesting that dynamic sorting, soil-forming processes and climatic influences, such as rainfall, altered the mineralogy and chemistry in these partially eolian deposits. Sistan is also an ideal site for studying dust storms and enrichment factors relative to crustal norms; the latter factors suggest that the dust is essentially of crustal rather than anthropogenic origin. SEM analyses of the samples indicated that airborne dust has rounded irregular, prismatic and rhombic shapes, with only the finer particles and a few examples of the coarser dust being spherical.

Author details

Alireza Rashki and C.J.deW. Rautenbach
Department of Geography, Geoinformatics and Meteorology,
Faculty of Natural and Agricultural Sciences, University of Pretoria, Pretoria,
South Africa
Department of Drylands and Desert Management, Faculty of Natural Resources and Environment,
Ferdowsi University of Mashhad, Mashhad,
Iran

Dimitris Kaskaoutis
Research and Technology Development Centre, Sharda University, Greater Noida, India

Patrick Eriksson
Department of Geology, Faculty of Natural and Agricultural Sciences, University of Pretoria, Pretoria, South Africa

15. References

[1] Mahowald, N.M., Bryant, R.G., Corral, J., and Steinberger, L. 2003. Ephemeral lakes and desert dust sources, Geophysical Research Letters,. 30, NO. 2, 1074

[2] Engelstaedter, S., Tegen, I., Washington, R., 2006. North African dust emissions and transport. Earth Science Reviews 79, 73-100.

[3] Koren, I., Y. J. Kaufman, R. Washington, M. C. Todd, Y. Rudich, J. V. Martins, and D. Rosenfeld 2006, The Bodele depression: a single spot in the Sahara that provides most of the mineral dust to the Amazon forest, Environmental Research Letters, 1(1).

[4] Baddock, M.C., Bullard, J.E., Bryant, R.G., 2009. Dust source identification using MODIS: A comparison of techniques applied to the Lake Eyre Basin, Australia. Rem. Sens. Environ. 113, 1511-1528.

[5] Orlovsky, L., Orlovsky, N., Durdyev, A. (2005) Dust storms in Turkmenistan. J Arid Environ 60:83–97

[6] Breckle, S.W., Wucherer,W., Liliya A. Dimeyeva, L.A., Nathalia P. Ogar, N.P. 2012. Aralkum - A Man-Made Desert: The Desiccated Floor of the Aral Sea (Central Asia), Springer, pp: 486

[7] Reheis M (1997) Dust deposition of Owens (dry) Lake, 1991–1994: preliminary findings. J Geophys Res 102:25999–26008

[8] Reheis, M., Budahn, J.R., Lamothe,P.J., and Reynolds, R.L.,, 2009. Compositions of modern dust and surface sediments in the Desert Southwest, United States, Journal Of Geophysical Research, 114, F01028, doi:10.1029/2008JF001009

[9] Whitney, J. W., 2006. Geology, Water, and Wind in the Lower Helmand Basin, Southern Afghanistan U.S. Geological Survey, Reston, Virginia, Retrieved 2010-08-31

[10] United Nations Environment Programme (UNEP). 2006. History of Environmental Change in the Sistan Basin Based on Satellite Image Analysis:1976 – 2005. P: 60

[11] Miri A, Moghaddamnia A, Pahlavanravi A, Panjehkeh N (2010) Dust storm frequency after the 1999 drought in the Sistan region, Iran. Clim Res 41:83-90

[12] Rashki, A., Kaskaoutis, D.G., Rautenbach, C.J.deW., Eriksson, P.G.,Giang, M, Gupta, P., 2012b. Dust storms and their horizontal dust loading in the Sistan region, Iran. Aeolian Research doi:10.1016/j.aeolia.2011.12.001

[13] IPCC, (Intergovernmental Panel on Climate Change), 2001. Climate Change 2001: The Scientific Basis. In Contribution of Working Group I to the Third Assessment Report of the Intergovernmental Panel on Climate. J.T. Houghton et al.; Eds, Cambridge Univ. Press, New York, USA.

[14] IPCC, 2007. Climate Change 2007: Synthesis Report. Contribution of Working Groups I, II and III to the Fourth Assessment Report of the Intergovernmental Panel on Climate Change. In: Core Writing Team, Pachauri, R.K., Reisinger, A. (Eds.), Geneva, Switzerland, p. 104.

[15] Tegen, I., Fung, I., 1994. Modeling of mineral dust in the atmosphere: sources, transport, and optical thickness. J. Geophys. Res. 99, 22897–22914.

[16] Tegen, I., Lacis, A.A., Fung, I., 1996. The influence on climate forcing of mineral aerosols from disturbed soils. Nature, 380, 419-422.

[17] Dunion, J.; Velden, C. 2004. The impact of the Saharan air layer on Atlantic tropical cyclone activity. Bull. Amer. Meteor. Soc. 85, 353-365.

[18] Prasad, A.K., Singh, S., Chauhan, S.S., Srivastava, M.K., Singh, R.P., Singh, R., 2007. Aerosol radiative forcing over the Indo-Gangetic Plains during major dust storms. Atmos. Environ. 41, 6289-6301.

[19] Singh, R.P., Prasad, A.K., Kayetha, V.K., Kafatos, M., 2008. Enhancement of oceanic parameters associated with dust storms using satellite data. J. Geophys. Res., 113, C11008, doi:10.1029/2008JC004815.

[20] Patadia, F., Yang, E.-S., Christopher, S.A., 2009. Does dust change the clear sky top of atmosphere shortwave flux over high surface reflectance regions? Geophys. Res. Lett., 36, L15825, doi:10.1029/2009GL039092.

[21] Mahowald, N., Baker, A., Bergametti, G., Brooks, N., Duce, R., Jickells, T., Kubilay, N., Prospero, J., Tegen, I., 2005. Atmospheric global dust cycle and iron inputs to the ocean. Global Biogeochem. Cycles Vol.19 (No.4), GB4025. doi:10.1029/2004GB002402.

[22] Claquin T, Schulz M, Balkanski Y, Boucher O (1998) Uncertainties in assessing radiative forcing by mineral dust. Tellus Ser B – Chem Phys Meteorol 50: 491–505

[23] Broecker, W.S., 2000. Abrupt climate change: causal constraints provided by the paleoclimate record. Earth Science Reviews 51, 137–154.

[23] Nriagu, J.O., and Pacyna, J.M. 1988. Quantitative assessment of worldwide contamination of air, water and soils with trace metals. Nature, 333: 134–139

[25] Husar, R.B., Prospero, J.M., Stowe, L.L., 1997. Characterization of tropospheric aerosols over the oceans with the NOAA advanced very high resolution radiometer optical thickness operational product. Journal of Geophysical Research 102, 16,889–16,909.

[26] Nriagu, J.O., 1988. A salient epidemic of environmental metal poisoning? Environmental Pollution 50, 139–161.

[27] Dockery, D., Pope, C.A., Xiping, X., Spengler, J., Ware, J., Fay, M., Ferris, B., Spiezer, F., 1993. An association between air pollution and mortality in six US cities. New England Journal of Medicine 329 (24), 1753–1759.

[28] Dockery, D., Pope, A., 1996. Epidemiology of acute health effects: summary of time-series studies. In: Particles in Our Air: Concentrations and Health Effects (Wilson R, SpenglerJD, eds). Harvard University Press, Cambridge, MA, 123-147.

[29] Pope, C. A., 2000. Epidemiology of fine particulate air pollution and human health: Biologic mechanisms and who's at risk?, Environmental Health Perspectives, 108, 713-723.

[30] Schwartz J. 2004. Air pollution and children's health. Pediatrics 113:1037-1043.

[31] Pozzi,R., B.D. Berardis, B.D., Paoletti, L., Guastadisegni, C., 2005. Winter urban air particles from Rome (Italy): effects on the monocytic–macrophagic RAW264.7 cell line, Environ. Res. 99: 344–354.

[32] Chakra, O.R.A., Joyeux, M., Nerriere, E., Strub, M.P., Zmirou-Navier, D., 2007. Genotoxicity of organic extracts of urban airborne particulatematter: an assessment within a personal exposure study, Chemosphere 66:1375–1381.

[33] Brook, R.D., Urch, B., Dvonch, J.T., Bard, R.L., Speck, M., Keeler, G., Morishita, M., Marsik, F.J., Kamal, A.S., Kaciroti, N., Harkema, J., Corey, P., Silverman, F., Gold, D.R., Wellenius, G., Mittleman, M.A., Rajagopalan, S., and Brooky, J.R., 2009. Insights into the mechanisms and mediators of the effects of air pollution exposure on blood pressure and vascular function in healthy humans. Hypertension, 54(3), 659-667.

[33] Sivagangabalan, G., Spears, D., Masse, S., Urch, B., Brook, R.D., Silverman, F., Gold, D.R., Lukic, K.Z., ; Speck, M., Kusha, M., Farid, T., Poku, K., Shi, E., Floras, J., Nanthakumar, K., 2010. Mechanisms of Increased Arrhythmic Risk Associated With Exposure to Urban Air Pollution. Circulation, 122, A17901

[35] Bhaskaran ,k. Wilkinson, p and smeeth, L., 2011. Cardiovascular consequences of air pollution: what are the mechanisms? Heart, 97, 519-520.

[36] Nastos, T., Athanasios. G., Michael, B., Eleftheria, S.R., Kostas, N.P., 2010. Outdoor particulate matter and childhood asthma admissions in Athens, Greece: a time-series study. Environmental Health , 9:45, 1-9.

[37] Wilson, A. M.; Salloway, J. C.; Wake, C. P.; Kelly, T., 2004. Air pollution and demand for hospital services: A review. Environ. Int., 30, 1109-1018

[38] Larney, F. J., Leys, J. F., Muller, J. F., & McTainsh, G. H. (1999). Dust and endosulfan deposition in cotton-growing area of Northern New South Wales, Australia. Journal of Environmental Quality, 28, 692–701.

[39] Lioy, P. J., Freeman, N. C. G., & Millette, J. R. 2002. Dust: A metric for use in residential and building exposure assessment and source characterization. Environmental Health Perspectives, 110, 969–983.

[40] Wood, W. W., & Sanford, W. E. (1995). Eolian transport, saline lake basins and groundwater solutes. Water Resources Research, 31, 3121–3129.

[41] Ganor, E., Foner, H.A., & Gravenshorst, G. (2003). The amount and nature of the dust on Lake Kinneret (the Sea of Galilee), Israel: flux and fractionation. Atmospheric Environment, 37, 4301–4315.

[42] Lawrence, C.R. and Neff, J.C. 2009. The contemporary physical and chemical flux of aeolian dust: A synthesis of direct measurements of dust deposition. Chemical Geology 267: 46-63.

[43] Chow, J. C., Watson, J. G., Ashbaugh, L. L., & Magliano, K. L. (2003). Similarities and differences in PM10 chemical source profiles for geological dust from the San Joaquin Valley, California. Atmospheric Environment, 37, 1317– 1340.

[44] Engelbrecht J.P, McDonald E.V, Gillies, J.A, Jayanty RKM, Casuccio, G., Gertler, A.W. 2009, Characterizing mineral dusts and other aerosols from the Middle East—Part 1: Ambient sampling.Inhalation Toxicology 21:297 -326

[45] Mishra, S.K., Tripathi, S.N., 2008. Modeling optical properties of mineral dust over the Indian Desert. J. Geophys. Res., 113, D23201, doi:10.1029/2008JD010048.
[46] Wilson, W.E., Chow, J.C. Claiborn, C. Fusheng, W. Engelbrecht, J. and Watson, J.G., 2002, Monitoring of particulate matter outdoors. Chemosphere, 49, 1009–1043
[47] Thurston, G.D., Spengler, J.D., 1985, A quantitative assessment of source contributions to inhalable particulate matter pollution in metropolitan Boston. Atmospheric Environment, 19, 9–25.
[48] Biscaye, P. E., & Grousset, F. E. (1998). Ice-core and deep-sea records of atmospheric dust. In A. Busacca (Ed.), Dust aerosols, loess soils, and global change (pp. 101–103). College Agric. Home Econ. Misc. Publ. MISC0190 (1998). Pullman, WA: Washington State Univ.
[49] Shaw, G. E. (1980). Transport of Asian desert aerosol to the Hawaiian Islands. Journal of Applied Meteorology, 19, 1254–1259.
[50] Goudie, A.S., Midelton, N.J., 2006. Desert dust in the global system, Springer. 2006, pp287.
[51] Alam, K., Qureshi, S., Blaschke, T., 2011. Monitoring Spatio-temporal aerosol patterns over Pakistan based on MODIS, TOMS and MISR satellite data and a HYSPLIT model. Atmos. Environ., 45, 4641-4651.
[52] Rashki, A., Rautenbach, C.J.deW., Eriksson, P.G., Kaskaoutis, D.G., Gupta, P., 2012a. Temporal changes of particulate concentration in the ambient air over the city of Zahedan, Iran. Air Quality, Atmosphere & Health. DOI: 10.1007/s11869-011-0152-5
[53] Miri, A., Ahmadi, H., Ghanbari, A., Moghaddamnia, A., 2007. Dust Storms Impacts on Air Pollution and Public Health under Hot and Dry Climate. Int. J. Energy and Environ. 2, 1.
[54] Selinus, 2010, Physics and modelling of wind erosion, springer
[55] Ranjbar, M., and Iranmanesh, F. 2008. Effects of "Drought" on "Wind Eroding and Erosion" in Sistan Region with use of Satellite Multiple Images. WSEAS, ISSN: 1792-4294.
[56] Middleton, N. J., 1986. Dust storms in the Middle East. J. Arid Environ. 10, 83-96.
[57] Esmaili, O and Tajrishy, M, 2006, Results of the 50 year ground-based measurements in comparison with satellite remote sensing of two prominent dust emission sources located in Iran, Proc. SPIE 6362, 636209; http://dx.doi.org/10.1117/12.692989
[58] Moghadamnia, A., Ghafari, M.B., Piri, J., Amin.S., Han. D., 2009. Evaporation estimation using artificial neural networks and adaptive neuro-fuzzy inference system techniques. Adv. Water Resources 32, 88–97.
[59] British Geological Survey; http://bgs.ac.uk/
[60] Tirrul, R., Bell, I. R., Griftis, R. J., Camp, V. E., 1983. The Sistan suture zone of eastern Iran. Bull. of Geological Soc. of America, 94, 134-150.
[61] Wittekindt, Hans, and Weippert, D., compilers, 1973, Geologische Karte von Zentral-und Sudafghanistan: Hannover, Bundesanstalt fur Bodenforschung, 4 sheets, scale 1:500,000

[62] O'Leary, D.W., and Whitney, J.W., 2005a, Geological map of quadrangles 3062 and 2962, Charbuiak (609), Khannesin (610), Gawdezereh (615) and Galach (616), Afghanistan: U.S. Geological Survey Open-File Report 2005–1122A, scale 1:250,000.

[63] O'Leary, D.W., and Whitney, J.W., 2005b, Geological map of quadrangles 3164, Lashkargah (605) and Kandahar (606), Afghanistan: U.S. Geological Survey Open-File Report 2005–1119A, scale 1:250,000.

[64] Barlow, Matthew, Cullen, H., and Lyon, B., 2002, Drought in central and southwest Asia: La Niña, the warm pool, and Indian Ocean precipitation: Journal of Climate, v. 15, p. 697–701.

[65] Partow, Hassan, 2003, Sistan oasis parched by droughts, in Atlas of global change: United Nations Environmental Programme, Oxford University Press, p. 144–145.

[66] Ekhtesasi, M.R., Daneshvar, M.R., Abolghasemi, M., Feiznia, S., and Saremi Naeini, M.A. Measurement and Mapping of Aeolian Sand Flowthrough Sediment Trap Method (Case Study: Yazd-Ardakan Plain), Journal of the Iranian Natural Res., Vol. 59, No. 4, 2007, pp. 773-781

[67] Ekhtesasi, M.R., (2009). National project of monitoring of wind erosion and sand storm in Iran, forests and range and watershed organization of Iran (Persian language)

[68] Rietveld H.M. 1969. A profile refinement method for nuclear and magnetic structures. J. ppl. Crystallogr.2:65–71.

[69] Sturges, W.T., Harrison, R.M. , Barrie L.A., 1989. Semi-quantitative XRD analysis of size fractionated atmospheric particles, Atmospheric Environment, 23 , 1083–1098

[70] Caquineau S, Magonthier MC, Gaudichet A, Gomes L. 1997. An improved procedure for the X-ray diffraction analysis of low-mass atmospheric dust samples. Eur. J. Mineral. 9: 157–166.

[71] Zarasvandi, A., 2009, Environmental impacts of dust storms in the Khuzestan province, Environmental Protection Agency (EPA) of Khuzestan province, Internal Report, 375p

[72] Zarasvandi,A., Carranza, E.J.M., Moore3, F., Rastmanesh, F. Spatio-temporal occurrences and mineralogical-geochemical characteristics of airborne dusts in Khuzestan Province (southwestern Iran), Journal of Geochemical Exploration, 111, 3, 138–151

[73] Hossenzadeh, S.R., 1997 One hundred and twenty days winds of Sistan. Iran Iranian Journal of Research Geography 46,103–127

[74] Goudie, A.S., Middleton, N.J., 2000. Dust storms in south west Asia. Acta Universitatis Carolinae, Supplement 73-83.

[75] Prasad, A. K.; Singh, R. P. & Kafatos, M. (2006), Influence of coal based thermal power plants on aerosol optical properties in the Indo-Gangetic basin, Geophysical Research Letters, 33(5).

[76] Kaskaoutis, D. G., Kambezidis, H. D.,Nastos, P. T., and Kosmopoulos, P. G., 2008. Study on an intense dust storm over Greece. Atmospheric Environment, 42, 6884-6896.

[77] Adamopoulos, A.D., Kambezidis, H.D., Kaskaoutis, D.G., Giavis, G., 2007. A study of particle size in the atmosphere of Athens, Greece retrieved from solar spectral measurements. Atmos. Res. 86, 194-206.

[78] Goudie, A. S., and Middleton.N.J., 2001. Saharan dust storms: nature and consequences. Earth-Science Reviews 56: 179–204.

[79] Knippertz, P., Ansmann, A., Althausen, D., et al., 2009. Dust mobilization and transport in the northern Sahara during SAMUM 2006 - A meteorological overview. Tellus B 61, 12-31.

[80] Zhang, D.E., 1985. Meteorological characteristics of dust fall in China since the historic times. In: Liu, T.S. (Ed.), Quaternary Geology and Environment of China. China Ocean Press, Beijing, pp. 45–56

[81] Offer, Z.Y., Goossens, D. 2001. Airborne particle accumulation and composition at different locations in the Negev desert, Zeitschrift für Geomorphologie, 45 (2001), pp. 101–120

[82] Dong, Z., Man, D., Luo, W., Qian, Q., Wang, J., Zhao, M., Liu, Sh., Zhu, G., Zhu, Sh. 2010. Horizontal aeolian sediment flux in the Minqin area, a major source of Chinese dust storms, Geomorphology 116 58–66

[83] Zhao, M., Zhan, K.J., Qiu, G.Y. Fang, E.T., Yang, Z.H., Zhang, Y.C., Ai De Li, A.D. 2011. Experimental investigation of the height profile of sand-dust fluxes in the 0–50-m layer and the effects of vegetation on dust reduction, Environ Earth Sci, 62:403–410

[84] Zhang, Z., Dong. Z., and Zhao. A. 2011. The characteristics of aeolian sediment flux profiles in the south-eastern Tengger Desert, Sedimentology (2011) 58, 1884–1894

[85] Zender, C.S., Miller, R.L., Tegen, I., 2004. Quantifying mineral dust mass budgets: terminology, constraints, and current estimates. EOS, Transactions, American Geophysical Union 85 (48), 509–512.

[86] Environmental Protection Agency (EPA), 1999. Guideline for reporting the daily air quality-air quality index (AQI). EPA-1999-454/R-99-010.

[87] Mohan, M., Kandya, A., 2007. An analysis of the annual and seasonal trends of Air Quality Index of Delhi. Environ. Monit. Assess. 131, 267–277.

[88] Larissi, I.K., Antoniou, A., Nastos, P.T., Paliatsos, A.G., 2010a. The role of wind in the configuration of the ambient air quality in Athens, Greece. Fres. Environ. Bull. 19, 1989-1996.

[89] Ozer, P., Bechir, M., Laghdaf, O.M., Gassani, J., 2006. Estimation of air quality degradation due to Saharan dust at Nouakchott, Mauritania, from horizontal visibility data. Water Air Soil Pollut, 178:79–87

[90] Triantafyllou, A.G., Evagelopoulos, V., Zoras, S., 2006. Design of a web-based information system for ambient environmental data. Journal of Environmental Management, 80, 230-236.

[91] Mousavi, G., Nadafy, R.K., 2000. Comparative study of air quality in Tehran in 1997 and 1998, The third National Conference on Environmental Health. Kerman. 47-50(In Persian)

[92] Cheraghi, M., 2001. Evaluation and comparison of air quality in Tehran and Isfahan in 1999 and offering solutions to improve It, MSc thesis of Environment, Natural Resources Faculty of Tehran University, 150 Pages (In Persian)

[93] Ardakani, S.Q., 2006. Determine the air quality in Iran in (2004).Journals of Environmental Science and Technology, Volume 8, Number 4, winter, p. 38-33(In Persian)

[94] Bartzokas, A., Kassomenos, P., Petrakis, M., Celessides, C., 2004. The effect of meteorological and pollution parameters on the frequency of hospital admissions for cardiovascular and respiratory problems in Athens. Indoor and Built Environ. 13, 271-275.

[95] Samoli, E., Kougea, E., Kassomenos, P., Analitis, A., Katsouyanni, K., 2011. Does the presence of desert dust modify the effect of PM10 on mortality in Athens, Greece? Sci. Total Environ. 409, 2049-2054.

[96] Usher,C.R., Michel, A.E., VH Grassian, V.H. 2003 Reactions on mineral dust, Chemical Review, 103 (12) , 4883–4940

[97] Larssen, T., Carmichael, G.R., 2000. Acid rain and acidification in china: the importance of base cation deposition. Environmental Pollution 110 (1), 89–102.

[98] Muhs, D.R., Benedict, J.B., 2006. Eolian additions to late quaternary alpine soils, Indian Peaks Wilderness Area, Colorado Front Range. Arctic Antarctic and Alpine Research 38 (1), 120–130.

[99] Yang, X.P., Zhu, B.Q., White, P.D. 2007, Provenance of aeolian sediment in the Taklamakan Desert of western China, inferred from REE and major-elemental data. Quaternary International 175, 71–85.

[100] Sokolik, I.N., Toon, O.B., Bergstrom, R.W., 1998. Modeling the radiative characteristics of airborne mineral aerosols at infraredwavelengths. Journal of Geophysical Research-Atmospheres 103 (D8), 8813–8826

[101] Erel,Y., Dayan,U., Rabi, R., Rudich,Y., Stein,M., 2006. Trans boundary transport of pollutants by atmospheric mineral dust. Environmental Science & Technology 40 (9), 2996–3005.

[102] Dentener, F.J.; Carmichael, G.R.; Zhang, Y.; Lelieveld, J.; Crutzen, P.J. 1996. Role of mineral aerosol as a reactive surface in the global troposphere. J Geophys. Res. 101(17): 22869-22889.

[103] Arnold, E., Merrill, J., Leinen, M., and King, J.: 1998. The effect of source area and atmospheric transport on mineral aerosol collected over the north pacific ocean, Global Planet Change, 18, 137–159

[104] Deer, W. A., Howie, R. A. and Zussman, J.: 1966, An Introduction to the Rock Forming Minerals, Longmans, pp. 528.

[105] Schütz,L., Sebert,M., 1987, Mineral aerosols and source identification, Journal of Aerosol Science, 18 (1) , pp. 1–10

[106] Reheis, M. C., and Kihl, R., 1995, Dust deposition in southern Nevada and California, 1984–1989: Relations to climate, source area, and source lithology: Journal of Geophysical Research, v. 100, p. 8893–8918.

[107] Wedepohl, K.H., 1971. Environmental influences on the chemical composition of shales and clays. In: Ahrens, L.H., Press, F., Runcorn, S.K., Urey, H.C. (Eds.), Physics and Chemistry of the Earth. Pergamon, Oxford, UK, pp. 307–331

[108] Clarke, F. W., 1924. Bull. U.S. geol. Surv., 700, p. 29.

[109] Gromet, L P, Dymek, R.F., Haskin, L.A., and Korotev, R.L. 1984) The "North American shale composite": Its compilation, major and trace element characteristicsG. eochimica et CosmochimicaA cta, 48,2469- 2482

[110] Talbot M.R. and Allen P.A. 1996. Lakes. in Sedimentary Environments: Reading H.G. (ed), Processes, Facies and Stratigraphy, Blackwell: Oxford, 83–124.

[111] Kreutz, K. and Sholkovitz, E. 2000. Major element, rare earth element, and sulfur isotopic composition of a high-elevation firn core: Sources and transport of mineral dust in central Asia. Geochemistry, Geophysics, Geosystems 1(11).1525-2027.